

CELL SENSING ON STRAIN-STIFFENING SUBSTRATES
IS NOT FULLY EXPLAINED
BY THE NONLINEAR MECHANICAL PROPERTY

A Thesis
Submitted to the Faculty
of the
WORCESTER POLYTECHNIC INSTITUTE
in partial fulfillment of the requirements for the
Degree of Master of Science
in
Biomedical Engineering
by

Mathilda S. Rudnicki

May 2012

APPROVED:

Kristen L. Billiar, Ph.D
Associate Professor
Department of Biomedical
Engineering
Thesis Advisor

Glenn R. Gaudette, Ph.D
Associate Professor
Department of Biomedical
Engineering
Committee Member

Raymond L. Page, Ph.D
Assistant Professor
Department of Biomedical
Engineering
Committee Member

Acknowledgements

I would like to extend my sincere gratitude to my advisor, Prof. Kristen Billiar; thank you for accepting me as your student. Your passion for learning, teaching, and problem-solving, and accepting challenges is very much an inspiration to me.

Many thanks to my committee members, Prof. Glenn Gaudette and Prof. Raymond Page, as well as Prof. George Pins, for your time spent discussing and refining the broad themes and small details of my project.

A warm thank you to Vicki Huntress for teaching me all I know about the confocal microscope, and for spending numerous hours figuring out just what it is we are looking at.

To Heather Cirka and Mehmet Kural, and the members of the Gaudette, Pins, and Rolle labs, thank you for your troubleshooting assistance, imparting your knowledge of the lab, and your camaraderie.

Thank you to Mom, Jenn, Colin, and Andrew for all of your encouraging words and your cheerful support.

Finally, thank you to my late father, to whom this work is dedicated.

Abstract

Cells respond to their mechanical environment by changing shape and size, migrating, or even differentiating to a more specialized cell type. A better understanding of the response of cells to surrounding cues will allow for more targeted and effected designs for biomedical applications, such as disease treatment or cellular therapy.

The spreading behavior of both human mesenchymal stem cells (hMSCs) and 3T3 fibroblasts is a function of substrate stiffness, and can be quantified to describe the most visible response to how a cell senses stiffness. The stiffness of the substrate material can be modulated by altering the substrate thickness, and this has been done with the commonly-used linearly elastic gel, polyacrylamide (PA). Though easy to produce and tune, PA gel does not exhibit strain-stiffening behavior, and thus is not as representative of biological tissue as fibrin or collagen gel. Fibroblasts on soft fibrin gel show spreading similar to much stiffer linear gels, indicating a difference in cell stiffness sensing on these two materials.

We hypothesize cells can sense further into fibrin and collagen gels than linear materials due to the strain-stiffening material property. The goal of this work is to compare the material response of linear (PA) and strain-stiffening (fibrin, collagen gel) substrates through modulation of effective stiffness of the materials. The two-step approach is to first develop a finite element model to numerically simulate a cell contracting on substrates of different thicknesses, and then to validate the numerical model by quantifying fibroblast spreading on sloped fibrin and collagen gels.

The finite element model shows that the effective stiffness of both linear and nonlinear materials sharply increases once the thickness is reduced below $10\mu\text{m}$. Due to the strain-stiffening behavior, the nonlinear material experiences a more drastic increase in effective stiffness at these low thicknesses. Experimentally, the gradual response of cell area of HLF and 3T3 fibroblasts on fibrin and collagen gels is significantly different ($p < 0.05$) from these cell types on PA gel. This gradual increase in area as substrate thickness decreases was not predicted by the finite element model. Therefore, cell spreading response to stiffness is not explained by just the nonlinearity of the material.

Table of Contents

Acknowledgements	i
Abstract.....	ii
Introduction.....	1
Background.....	3
Cell responses to stiffness	3
Effect of substrate thickness.....	5
Quantification of stiffness sensing	6
Methods	11
Finite Element	11
Experimental	14
Results	19
Finite Element	19
Experimental	25
Discussion.....	28
Finite Element	28
Experimental	32
Conclusion	35
References.....	36
APPENDIX.....	38
A brief introduction to Finite Element Analysis	38
Details on the development of the Finite Element Model.....	39
Stress and strain distributions.....	46
Area prediction from FE results	51
Experimental details	53

Introduction

The stiffness of the substrate on which a cell grows can dramatically influence the behavior of the cell. These affected behaviors include morphology, migration, differentiation, and proliferation and vary between cell types. With the behavior of cells so affected by substrate rigidity, it is critical to take the mechanical properties of cell substrates into consideration when studying cells. Furthermore, a greater understanding of the effects of tissue rigidity on cell behavior can provide vital information in developing tissue engineering solutions that are aimed to treat disease or provide cellular therapy.

The differentiation, apoptosis level, and amount of spreading of cells are influenced by the stiffness of the substrate on which the cells are cultured. When grown in calcification media, valve interstitial cells develop calcified bone-like nodules on soft collagen gel, but have more apoptosis and differentiation to contractile myofibroblasts when on stiffer collagen gel (Yip et al. [1]). Similarly, adult neural stem cells grown in differentiation media respond to stiffness by differentiating into neurons (soft) or glia (stiff) (Saha et al. [2]). Annulus fibrosus cells harvested from the lumbar spine of rats and cultured on polyacrylamide (PA) gels of various stiffnesses have a more spread morphology and lower levels of apoptosis on stiffer substrates (Zhang et al. [3]). This lower level of apoptosis on soft PA gel is also seen in 3T3 fibroblasts, though apoptosis of transformed version of these cells is not affected by substrate stiffness (Wang et al. [4]). Ulrich et al. [5] found that the spreading, migration, and proliferation of glioblastoma multiforme cells are strongly dependent on the rigidity of the substrate.

It is agreed upon that cells can sense the mechanical properties, specifically the stiffness, of their environment; however, because we cannot simply ask a cell what it is feeling, we must interpret this sensing by quantifying cell and substrate behavior. Maloney et al. [6] provide several definitions of a critical substrate thickness where a cell can sense the effects of a rigid boundary, including the depth at which a certain strain exists, or a thickness that maintains a particular surface displacement due to applied traction. A finite element model developed by Sen et al. [7] concluded, by measuring the strain field

between contracting cells, that hMSCs can sense a nearby cell if the cells are within one cell-length apart. Experimental results of hMSCs on PA gel by Buxboim et al. [8] agree with the aforementioned finite element model. In contrast, Winer et al. [9] found that hMSCs and 3T3 fibroblasts on fibrin gel can deform the gel up to five cell-lengths away, concluding that cells respond to the nonlinear substrate properties differently than they do to those of a linear substrate. This larger scale of sensing on a nonlinear substrate is shown by Leong et al. [10], where hMSCs on collagen gel spread on gels much thicker than those of Buxboim et al. [8].

There is an evident difference in how a cell responds to not just the substrate stiffness, but to the stress-strain relationship of the substrate. PA gel is an easily-produced and easily-tuned linearly elastic material on which cell sensing is being studied. However, materials with this linear property are not representative of biological tissues. Therefore, the next step in understanding cell sensing is to study the cell response to substrate thickness on a more representative tissue analog.

The strain-stiffening material property of fibrin and collagen gels lead to the hypothesis that as substrate thickness decreases, cells cultured on these nonlinear materials will sense the rigid boundary before cells cultured on PA gel. To test this hypothesis, the approach has two steps:

1. Develop a finite element model to quantify the increase of effective stiffness with decreasing thickness linear and nonlinear substrates.
2. Experimentally validate the finite element results with cells cultured on thin nonlinear gels that are sloped for material consistency and for testing multiple thicknesses simultaneously.

This approach will advance our knowledge of cell sensing, will lend to better understanding of cell-substrate mechanics, and aid in more rational design of engineered tissue solutions.

Background

Cell responses to stiffness

Cellular responses to cues from the surroundings allow organisms to adapt and survive in a wide range of environments. Topographical cues in the environment can lead to cell alignment and migration, thereby removing the dependence on chemical factors to obtain a particular cell response (Oakley et al. [11]). Cell response to the chemical environment, such as growth factors, can be enhanced when used in combination with different substrate stiffnesses (Semler et al. [12]). Various cell types respond to substrate stiffness in different ways: hMSCs show polygonal morphologies similar to osteoblasts when cultured on stiff substrates (Engler et al. [13]), but on the softest material, undergo neuron branching (Flanagan et al. [14]); on medium-stiffness substrates, myoblasts form more striated myotubules after four weeks in culture than on softer or stiffer substrates (Engler et al. [15]). Fibroblasts have even been shown to migrate when encountering a stiffness gradient, preferring stiffer materials to soft (Lo et al. [16]).

The stiffness of various tissues found in the body range from under 1kPa to tens of kPa, as shown in Figure 1 (Buxboim et al. [8]).

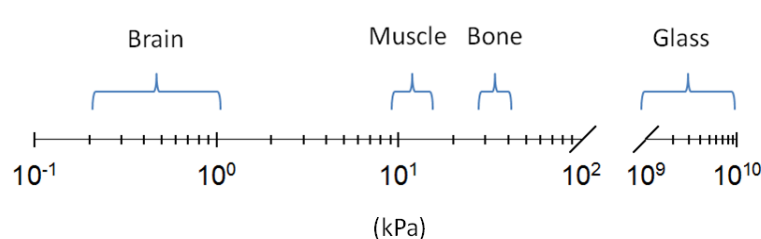


Figure 1. The stiffness of biological tissues spans over two orders of magnitude. Replotting of data from Buxboim et al. [8].

Different cell types respond and thrive - proliferate, migrate, apoptose as necessary for system function - at these different stiffnesses. In particular, fibroblasts have been shown to spread in response to substrates increasing in stiffness within this biologically-relevant range (Engler et al. [17], Yeung et al. [18], Solon et al. [19]). One of the more visible cellular responses to substrate stiffness is the area of the cells, and can be seen with staining the cytoskeleton or cytoplasm. Not only do cells on stiffer substrates have larger areas, but also feature more stress fibers, as seen by phalloidin staining of 3T3 fibroblasts, Figure

2(a). The location and prominence of the stress fibers may contribute to the varying traction that the cell applies to the substrate, as seen in Figure 2(b).

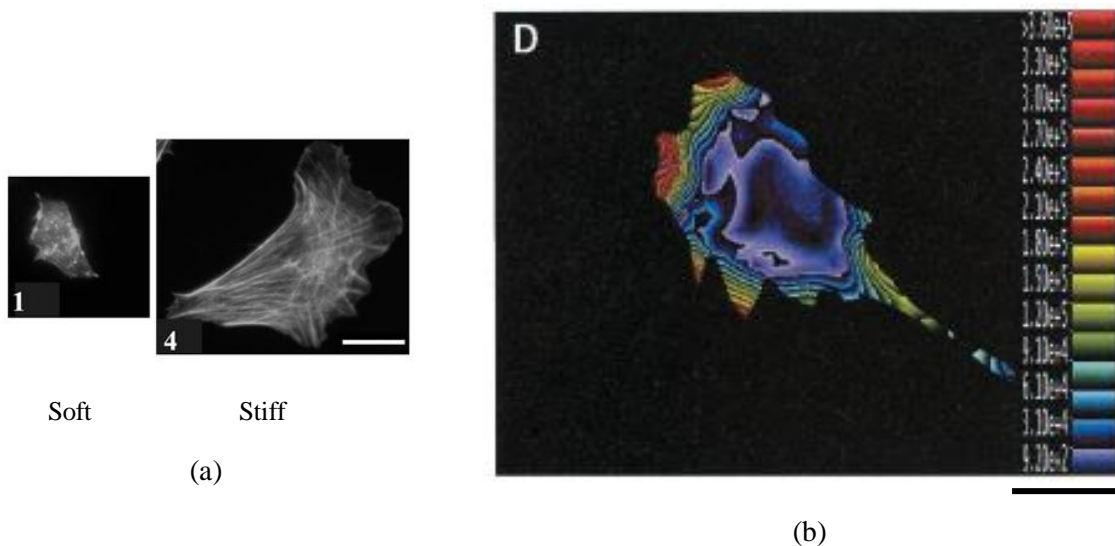


Figure 2. 3T3 Fibroblast spread morphology. (a) Fibroblasts on 1kPa PA gel (left) and glass (right); scale bar = 40 μ m. Solon et al. [19]. (b) Traction force microscopy of a migrating fibroblast on 2.8kPa PA gel; scale bar \approx 20 μ m; traction in dyn/cm² (10 dyn/cm² = 1Pa). Munevar et al. [20]. Reprinted with permission.

Interestingly, as seen in Figure 3, the cell spreading response of 3T3 fibroblasts (Solon et al. [19], Winer et al. [9]) is similar to that of hMSCs (Engler et al. [13]), cultured on the same PA substrate. Though these cell types are at different stages of differentiation, they exhibit similar spreading behavior on PA substrates of different stiffnesses.

PA gel has been a popular choice of substrate for studying cell response to substrate stiffness since Pelham and Wang [21] used this material to study cell locomotion and focal adhesions on substrates of various stiffnesses. In addition to being easily producible, the substrate is easily tuned to a specific stiffness, with Young's modulus ranging from 6Pa to 150kPa by following the general procedure specified by Yeung et al. [18]. The tunable stiffnesses allow for a range of simulated environments, from soft brain-like softness to calcification-like stiffness. Because cells will not bind to PA, there is neither compaction of the material nor burrowing as the cells are cultured, so the cultured cells are constrained to the two-dimensional environment.

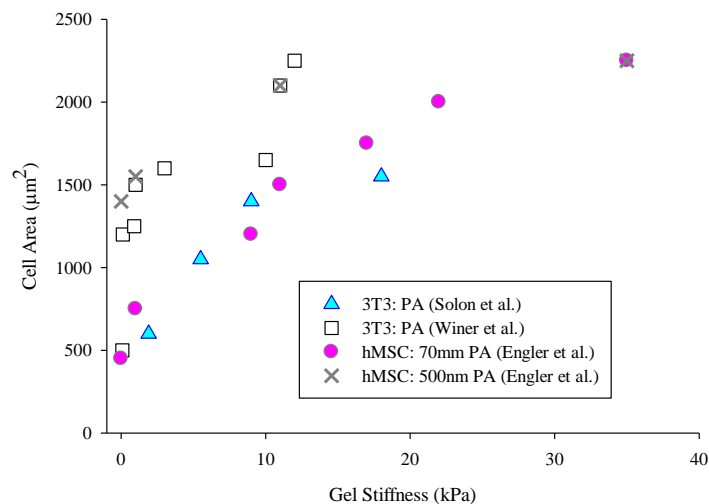


Figure 3. 3T3 fibroblasts and hMSCs respond to increasing substrate stiffness by spreading. The cells on the thickest PA gels (▲,●) respond similarly to gel stiffness, but cells on thin PA gels (X) are affected by the rigid boundary. Replotting of data from Solon et al. [19], Winer et al. [9], and Engler et al. [13].

The mechanism of cellular response to stiffness is beyond the scope of this work, thus this work focuses on comparison of cell stiffness sensing by quantifying the cellular spreading of fibroblasts.

Effect of substrate thickness

Defining the extent to which a cell senses stiffness leaves much room for interpretation. Maloney et al. [6] compiled several definitions of a critical depth where a cell senses a rigid boundary of the substrate. The definition used by this group, which modeled a focal adhesion displacing and distorting the surface of a substrate, considers this critical depth where the adhesion site displacement decays by a certain amount. Alternatively, Krishnan et al. [22] defined the critical thickness as the depth where the principal strain decays to $<0.1\%$. Under this definition, this group's finite element model indicated that a linearly elastic substrate with Young's modulus of 18kPa would have to be $3\mu\text{m}$ thick. The distribution of principal strain in substrates larger than $3\mu\text{m}$ would be entirely dissipated, and thus a cell would not be able to sense the rigid boundary. Increasing the stiffness to 1800kPa reduces this critical depth to $0.375\mu\text{m}$, implying that there is some dependence on material stiffness.

In an effort to change the stiffness that a cell senses but maintain substrate composition, several groups have experimented with modifying substrate thickness and observing the cell spreading behavior.

Cells cultured on thick and thin gels have been shown to present with different morphology due to the thickness of the substrate.

3T3 fibroblasts (Maloney et al. [6]) cultured on PA gel for 24 hours have a very similar response to human mesenchymal stem cells (Buxboim et al. [8]) on the linear substrate at the same time point. As the substrate thickness decreases, the cell area increases dramatically as substrates dip below $50\mu\text{m}$, as shown in Figure 4.

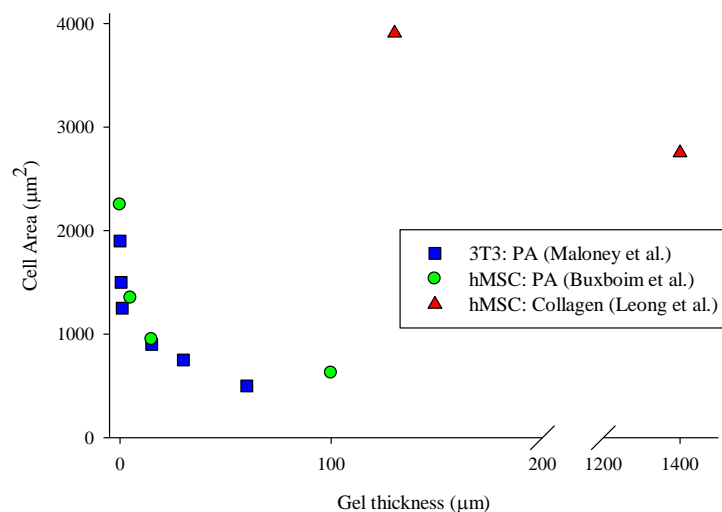


Figure 4. 3T3 fibroblasts and hMSCs respond to decreasing substrate thickness by spreading. When cultured on PA gel, these two cell types follow a similar curve. Though there are only two data points for hMSCs cultured on collagen, these cells spread on much thicker substrates than when cultured on PA gel. Replotting of data from Maloney et al. [6], Buxboim et al. [8], and Leong et al. [10].

This spreading is similar to that of cells on stiffer substrates; the thin substrate is *effectively* stiffer than the thick substrate. By culturing cells on collagen gel (3 mg/mL) rather than on PA gel, Leong et al. [10] saw much higher cell area of human mesenchymal stem cells with reduced substrate thickness compared to Maloney et al. [6] and Buxboim et al. [8]; though only two thicknesses were studied, cells on these collagen gels at a two day time point behave as if the gels were much thinner.

Quantification of stiffness sensing

Linear substrates

Finite element simulations provide a method of looking into a model during and after a series of events, and can be used to find areas of concern or to look at distributions of different variables. To

determine how far cells sense, Sen et al. [7] developed a model describing a linearly elastic gel on which sits a cell (hMSC), complete with cell membrane, cytoplasm, and nucleus. The model, as shown in Figure 5, is computationally simplified by defining an axis of symmetry through the center of the cell and then solving the two-dimensional model.

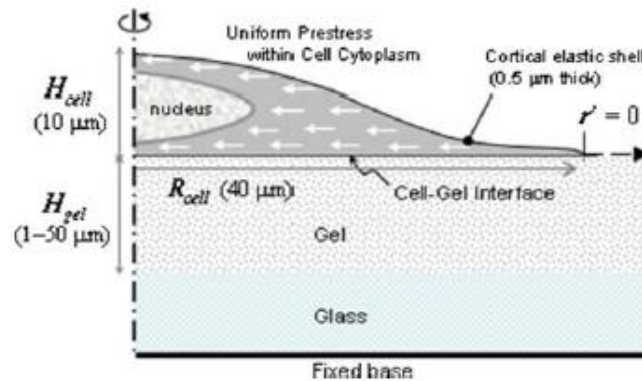


Figure 5. Schematic of the finite element model developed by Sen et al. [7]. The axisymmetric model features a rigid base, gel of variable stiffness, contracting cytoplasm, and non-contractile nucleus. Reprinted with permission.

The stiffnesses chosen by Sen et al. [7] encompass the range of biological tissue stiffnesses, as shown in Figure 1, from brain to osteal stiffnesses. The gel is defined wider than the cell to model an infinite plane, and the gel thickness ranges from 1–50 μm . By modeling a contracting cell at more thicknesses than done by Krishnan et al. [22], this model quantifies cell sensing with a critical thickness. The critical thickness, defined by fitting the gel surface displacement-gel thickness curve to a hyperbola, increases with increasing gel stiffness. A cell on a softer substrate has a smaller critical thickness, and therefore the rigid boundary is not seen until the gel is quite thin; as stiffness increases, the gel must get thicker to effectively hide the boundary from the cell.

In addition to determining the critical thickness, the finite element model used by Sen et al. [7] allowed this group to visualize the displacement and strain gradients throughout the substrate. To investigate the distance at which cells could sense one another, this group modeled two cells separated by various distances, as shown in Figure 6. By examining the strain field decay in the substrate between the cells, the group observed that the strain between cells at least once cell-length apart decays to $\sim 3.5\%$, and concluded that when cells are within one cell-length apart, the substrate is displaced enough to permit cell communication.

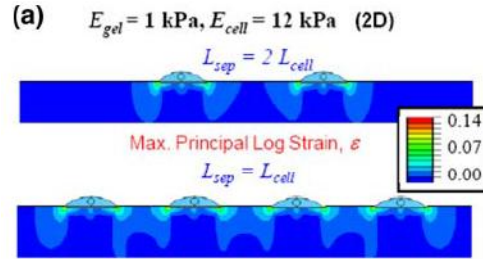


Figure 6. Sensing scale of finite element-modeled contracting cells on a linearly elastic substrate. Note that when the separation is two cell lengths, the strain field between the cells decays to zero (above). Placing the cells only one cell-length apart does not leave enough space for the strain to decay to zero (below). Thus, cells can be influenced by a nearby cell that is within one cell length away. Sen et al. [7]. Reprinted with permission.

To experimentally validate the model results, Buxboim et al. [8] cultured hMSCs on PA gels of different thicknesses to explore the critical thickness E where a cell can sense the rigid boundary. Instead of visualizing strain distributions, this group quantified the spreading area of individual cells at each thickness. With the cell area plotted with gel thickness, this group showed that area begins increasing once the gel thickness is brought below $20\mu\text{m}$, increasing by 50% between the 100 and $15\mu\text{m}$ data points. In addition, a fit of these data to an equation for hyperbolic decay showed the curvature parameter as just under $4\mu\text{m}$, as shown in Figure 7. Buxboim et al. [8] interpreted this parameter value of 3.4 as the thickness at which a cell can begin to see the rigid boundary. This critical thickness agrees with the sensing scale determined by the finite element model of Sen et al. [7].

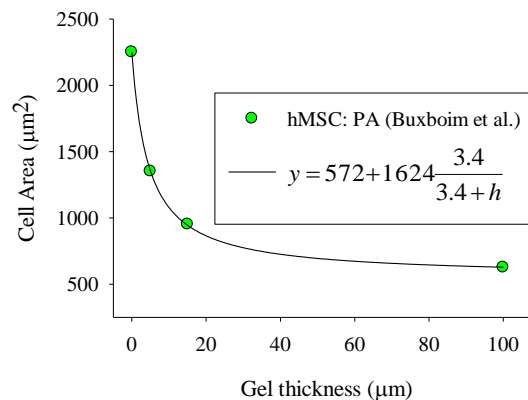


Figure 7. hMSCs cultured on 1kPa PA gel of various thicknesses. The fit to the hyperbolic decay defines the critical thickness as $3.4\mu\text{m}$, which is in agreement with the sensing scale of the finite element model of Sen et al. [7]. Replotting of data from Buxboim et al. [8].

Nonlinear substrates

A common way of defining materials used in construction and non-biological engineering is with a Young's modulus, or ratio of stress to strain in the material. The Young's modulus defines the linear elasticity of these materials: the material, if loaded under the yield stress or strain, will return to the original shape once unloaded before yielding, and will do so with a constant slope of the stress-strain curve. Biological materials, such as skin, brain tissue, and blood vessels, also exhibit elasticity but experience strain-stiffening and thus, cannot be easily defined with just a Young's modulus. As the material is strained, higher stress is required to strain the material further, similar to the amount of effort needed to inflate a balloon. In Figure 8, the stress required to bring the material to 50% strain is roughly 300Pa; straining the material an additional 30% requires an additional 600Pa.

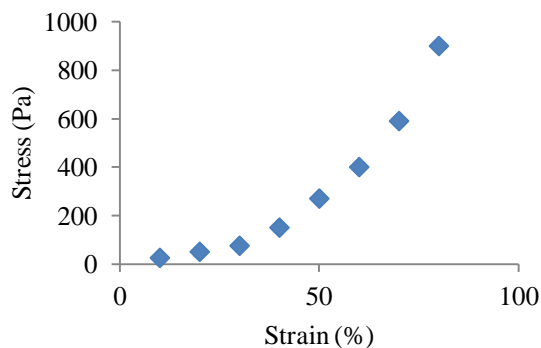


Figure 8. Stress-strain relationship of a 2mg/mL fibrin gel, as measured with rheometry, exhibiting strain-stiffening behavior. Replotting of data from Winer et al. [9].

In contrast to the short distances over which cells can sense on PA gels, Leong et al. [10] showed that spreading occurs on soft but thick collagen gel, as shown in Figure 4. Winer et al. [9] found that the cell area of fibroblasts cultured on a soft fibrin gel, with sub-kPa low-strain stiffness, was similar to that of fibroblasts cultured on a PA gel of relatively high stiffness, as shown in Figure 9. This behavior is also seen in hMSCs, and may indicate that the cells locally increase the stiffness of the nonlinear material and then spread as a result of this apparently stiffer substrate. By traction force microscopy, this group saw fibrin gel displacements on the order of several cell-lengths away. In the literature, there is a difference in

length scales of cells on nonlinear materials (Winer et al. [9], Leong et al. [10]) from cells on linear materials (Sen et al. [7], Buxboim et al. [8]). In addition to nonlinear materials better representing biological tissue than linear materials, the material difference may affect the ability to use the thickness to modulate stiffness, and warrants the further investigation of cell sensing on nonlinear substrates.

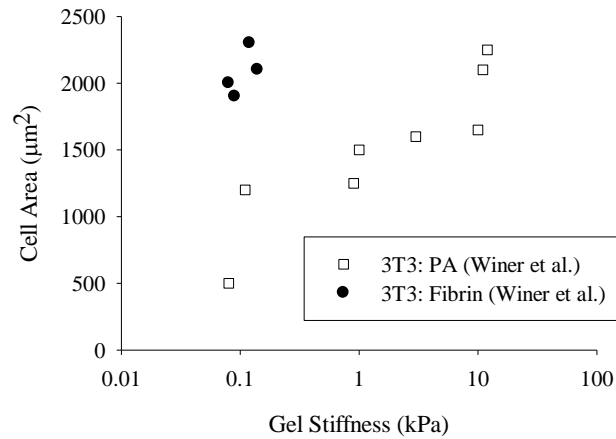


Figure 9. 3T3 fibroblasts cultured on PA gel increase in area as stiffness increases. When cultured on 2mg/mL fibrin gel, these cells spread as if on a much stiffer substrate. Replotting of data from Winer et al. [9].

Methods

Our approach for studying cell spreading behavior on a strain-stiffening (nonlinear) material is a two-step approach: first, a finite element model is developed to simulate a cell contracting on a substrate, and second, experimental work is done to quantify the area of cells on nonlinear substrates of different thickness.

The model developed in this work will put the focus on the response of a substrate to a cell-applied traction along a portion of the top surface. The displacement of the substrate due to this traction will allow us to calculate the effective stiffness of the material; a measure of the extent to which a cell can deform the substrate, and the effects of a rigid boundary under the substrate.

The model developed here has geometry and parameters different from published models, yet for validity, the linear model is tuned so that substrate response matches that of published finite element analyses. This validation is critical for the model when the material definition is changed from linearly elastic to nonlinear. The strain-stiffening behavior of the nonlinear material, which is based on rheological data of fibrin gel, is expected to show a different response (trend of effective stiffness versus gel thickness) from that of the linear material.

The experimental work employs sloped protein gels on which fibroblasts are cultured. The sloped gels allow the ligand density to remain the same throughout the sample, and also increase efficiency of data gathering by allows numerous substrate thicknesses within once sample.

Finite Element

Linearly elastic model development

The finite element model used in this research is based on the Sen et al. [7] model, with a simplified geometry based on that by Mehrotra et al. [23], which eliminates the complicated cell with internal stresses. The removal of the modeled cell simplifies the model definition and allows for more

efficient post-processing of the data by focusing on the response of the substrate, rather than on modeling the cell.

The geometry of the gel is based on geometry and loading from the model of Sen et al. [7] and Mehrotra et al. [23], respectively (see the Appendix, p39), and are shown in Figure 10.

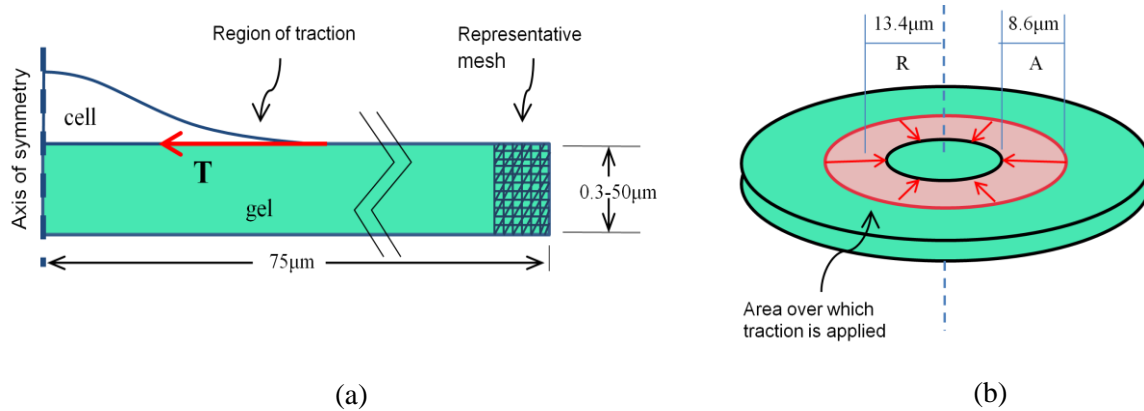


Figure 10. (a) Schematic of the finite element model: traction is applied to the top surface of a substrate. The lower boundary is fixed while the left boundary can move only vertically. Nine versions of the model are created in different thicknesses from 0.3-50 μm . The cell is shown for reference but is not modeled, allowing focus to be on the substrate response to a cell-applied traction. (b) Revolved about the axis, the model simulates a round cell applying traction along an annulus of given dimensions.

The width of the gel is semi-infinite (meaning the stresses and strains dissipate to zero); the lateral boundaries do not affect the deformation of gel in the area of applied traction. The thickness of the substrate ranges from 0.3 to 50 μm (0.3, 1, 2.5, 5, 10, 12, 15, 20, 50 μm), with the thickest gel considered to be infinite thickness, as seen by the cell. At the “infinite thickness” of 50 μm , the rigid boundary under the substrate does not affect the surface deformation, as seen by the very low strains (Appendix, p46). The axisymmetric model makes two assumptions: first, the cell is circular, thus allowing a computation-saving axisymmetric model to be analyzed; and second, the focal adhesion is modeled as a surface traction at the outer portion of the cell-gel interface, thus creating an annulus when the model is revolved about its axis of symmetry. The location of the traction is based on a study by Mehrotra et al. [23] that observes cell behavior on thin polyelectrolyte multilayers. This group calculated cell area and focal adhesion area by image analysis of highlighted areas in a region of interest with the assumption that cells are circular with focal adhesions toward the outer edge. As done by Mehrotra et al. [23], cell contraction is modeled with a constant traction along the focal adhesion area, thereby creating an annular ring of

inwardly directed traction. To ensure that this model produced results comparable to those that have been published, four stiffness values as per Sen et al. [7] were used in the linear finite element simulations. The stiffnesses range includes that of brain tissue (1kPa), the intermediate stiffness of muscle (5, 12kPa), and stiffer osteoids (40kPa). Finite element simulations of the model of “infinitely” thick substrate (50 μ m) were performed with various tractions to determine the level that produces displacements on the order of those done by Sen et al. [7].

Finite element simulations were performed using ABAQUS v6.8 (Providence, RI). CAX6M elements (6-node-modified quadratic axisymmetric triangular) were used, and elements ranged in number from 200 (for 0.3 μ m) to 8000 (for 50 μ m) per simulation. A Poisson’s ratio of 0.45 was used for all linear simulations.

The location of the cell-applied traction from the axis of symmetry (R) and the distance over which the traction is applied (A), as shown in Figure 11, is based on quantification data of 3T3 fibroblasts by Mehrotra et al. [23]. Parametric analyses different values for R and A were performed to determine the substrate response to larger or smaller cells (by changing R) and larger or smaller cell-substrate interface (by changing A).

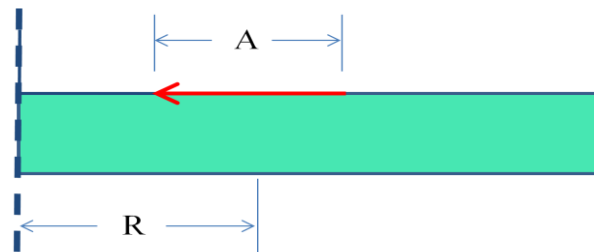


Figure 11. The size of the applied traction, A, and mean distance of the traction from the axis, R, are shown on the finite element substrate.

Strain-stiffening material definition and validation

The material definition used in the finite element model of this project is based on shear rheometry data of fibrin gel of 2mg/mL. The low-strain response of the fibrin gel was obtained with 2% oscillatory shear strain, while the high-strain response was obtained by bringing the gel to 100% strain

with the same angular velocity as the low-strain response (Winer et al. [9]). The data in this stress-strain relationship (shown in Figure 8) were fit to a third-order reduced polynomial model in ABAQUS with the following form:

$$W = C_{10}(I_I - 3) + C_{10}(I_I - 3)^2 + C_{10}(I_I - 3)^3 + \frac{1}{D_1} \quad (1)$$

where W is the strain energy per unit volume, I_I is the first strain invariant, and D_1 is a compressibility term. For details on the steps for validating the strain-stiffening material, see the Appendix, p39.

Simulating substrate response of cell contraction

Simulations were performed to analyze the effects of substrate thickness and cell-applied traction. Substrate thickness, as reported by Sen et al. [7], affects the strain distributions of a linear elastic substrate in such a way that cells may “feel” the very stiff underlying substrate. The substrate thickness in the simulations varied from 0.3 to 50 μm , stated previously. As the material definition of this model experiences strain-stiffening, simulations were performed with the cell-applied traction varying from 50Pa up to 600Pa. These values were chosen to capture the substrate responses at low and upper-mid range of strains while preventing element distortion and staying within the range of cell tractions found by Munevar et al. [20], Wang et al. [24], and Franck et al. [25].

Experimental

Gel mold design and sample preparation

Modulating the stiffness of a linearly elastic material, such as PA gel, is simply a matter of adjusting the polymerization components (see the Appendix, p53). Though nonlinear protein gels cannot be described by one stiffness value, adjusting the protein concentration can make the material overall stiffer or softer. However, cells cultured on protein gels of different concentrations are responding to the different mechanical properties of the material due to the increased ligand concentration, and the altered protein environment.

A method for producing a thin gel with an inclined surface was developed in this project. Rather than create multiple thin, constant-thickness gels of various thicknesses, this inclined gel method allows the study of cells on various thicknesses of the same material within the same sample.

The sloped substrate was created by sandwiching unpolymerized gel between two pieces of glass with a spacer on one side, as shown in Figure 12.

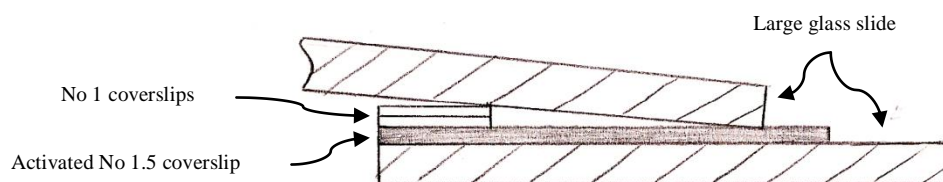


Figure 12. Schematic of the experimental setup for creating the sloped gel sample. The collagen or fibrin gel adheres to the activated No 1.5 coverslip and is formed into the sloped shape by the upper large glass slide that is weighted with a 50g object.

To create a sloped gel, the substrate must firmly attach to the bottom glass piece, yet separate easily from the top. The slides to which the gel should adhere firmly were activated as per Pelham and Wang (1997). Briefly, the glass is passed over an ethanol flame, exposed to 0.1N NaOH, and air dried. A thin coat of 3-aminopropyltrimethoxysilane is applied to the glass and incubated at room temperature for 5 minutes, and then the glass was rinsed in deionized H₂O. To activate the surface, 0.5% glutaraldehyde was then applied to the glass and incubated at room temperature for 30 minutes, and the slides were again rinsed, then air dried. To facilitate the removal of the collagen or fibrin gel from the top glass slide, Rain-X or Sigmacote may be applied to the glass. However, residual Rain-X was observed to affect the health of the cells, so the top glass slide was left untreated. An initial maximum thickness of 150 μ m is used to act as the substrate of infinite thickness. Based on finite element simulations that showed 50 μ m-thick gels as infinitely thick, this 150 μ m thickness will be sufficiently thick to show differences in cell area and can be created with readily available lab materials. To achieve this thickness, two No.1 coverslips (18x18mm, Electron Microscopy Sciences), each with approximate thickness of 150 μ m, were used as a spacer between the two glass pieces by attaching the coverslips to the bottom glass with silicone glue. The schematic of a finished sample ready for cell seeding is shown in Figure 13.

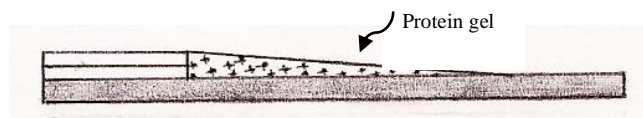


Figure 13. Schematic of the finished sample ready for cell seeding. Two samples are placed in a 100mm dish and the right side is propped up with two No 1 coverslips to ensure a level seeding surface.

See the Appendix, p53 for the testing of glass surface treatments.

Collagen gel samples were prepared in a cold room (4°C) to minimize polymerization during sample preparation. Collagen gel was prepared with acid-extracted rat tail tendon (RTT) collagen and polymerized with sodium hydroxide between glass slides at room temperature for approximately one hour. DMEM was added to the unpolymerized mixture to bring the final collagen concentration to ~4mg/mL. Fibrin gels were prepared at room temperature by polymerizing fibrinogen and thrombin with calcium. DMEM and HBSS were added to the unpolymerized mixture to bring the final fibrinogen concentration to ~4.5mg/mL. After 15min, the top glass slide was removed, and the gel was allowed to polymerize for an additional 45min. See the Appendix, p56 for protein gel protocols.

Cell culture

Human lung fibroblasts (HLF) and 3T3-J2 fibroblasts, graciously donated by Prof. George Pins, were cultured in DMEM with 10% FBS (HLF) or 10% BCS (3T3-J2) and 1% streptomycin/penicillin, and incubated at 10% CO₂. Samples were seeded at approximately 3000 cells/cm². To minimize effects of an incline, the end of the sample with the thinner substrate was propped up the appropriate amount to ensure a level substrate for the cells. To make sure the cell suspension remained atop the gel, rectangular frames cut from a thin silicone sheet (0.015", SM, MI) were placed on the gel immediately prior to cell seeding (see the Appendix, p59).

Cell staining

Cells were cultured overnight (~16hr) before fixing with 4% paraformaldehyde for 15 minutes. Following two five-minute rinses with PBS, cells were stained for F-actin with phalloidin (Invitrogen) and incubated for 30 minutes at 37 °C. Following three ten-minute rinses, nuclei were stained with Hoechst 33342 (Invitrogen) for 3-5 minutes and rinsed twice.

Cell imaging

In a first attempt to quantify the thickness of the substrate with the top slide removed, PA gel substrate samples were imaged from the side using an inverted microscope. This method captured only the edge of the gel, which is prone to drying and wrinkling. This method could not show cross sections of the gel at different areas of the sample, and thus, was abandoned.

Using the reflective properties of collagen and fibrin gels, the confocal microscope (Leica) was used in reflectance mode and in cross-section (XZY) mode. Below, fibers of a collagen droplet of 3 mg/mL RTT collagen are seen in , taken with a 40x oil objective.



Figure 14. Collagen fibers are visible in reflectance mode with a 40x oil objective on a confocal microscope.

In cross-section (XZY) and reflection mode, the confocal microscope produces images like the one shown in Figure 15(a). Since the microscope is an inverted style, the grayscale images are upside-down images of the sample (Figure 15(b)). The bright lines are the result of refractive index differences of the materials; the topmost line is between air and glass, then glass and collagen gel, etc. Due to these differences, the physical measurements of the coverslips do not agree with those from the confocal software (see the Appendix, p55). The network of the protein gel can be seen as a speckled pattern. The ratio of the micrometer-measured and the confocal-measured glass is roughly 1.5, which is the ratio of refractive indices of glass and air. This ratio was used to correct gel thickness measurements.

Due to the constraints of the confocal objective's working distance, an acrylic holder was designed to which gel substrates prepared on No. 1 ½ coverslips could be attached (see the Appendix, p54). These coverslips were activated as described above and attached to the acrylic holder by embedding into a continuous bead of rubber cement (Elmer's) and covered with mineral oil to prevent substrate dehydration or swelling. Cells were imaged with a Leica (Leica Microsystems GmbH, Germany) inverted confocal microscope using a 10x dry objective; controls were imaged with a Leica inverted fluorescent microscope using a Leica 10x dry objective. The gel samples were covered with mineral oil to prevent dehydration and swelling, and to visualize the top surface of the gel.

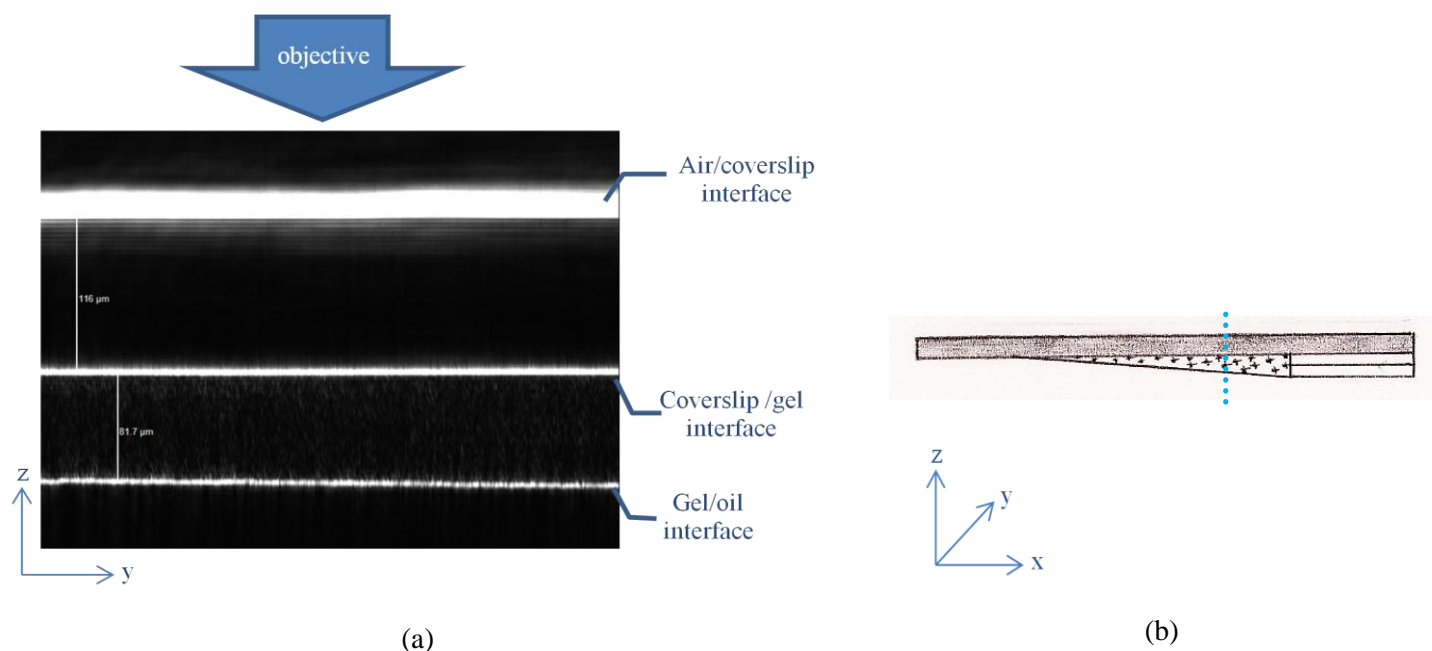


Figure 15. Due to its inverted setup, the cross-sectional images from the confocal microscope (a) are an upside-down version of the sample (b). The activated No. 1.5 coverslip is between the top and middle white lines, while the protein gel fibers (here, collagen) can be seen as the speckled pattern.

Cell area was quantified using ImageJ (NIH). The phalloidin images were thresholded to highlight the cells, and these images were visually compared to the original image to ensure the threshold level was acceptable. Upon review of images, only cells at least 50 μm away from the nearest cell were included in the quantification (see the Appendix, p60). This distance is chosen to balance minimizing spreading influence due to nearby cells with maintaining cell proximity seen in the natural environment.

Results

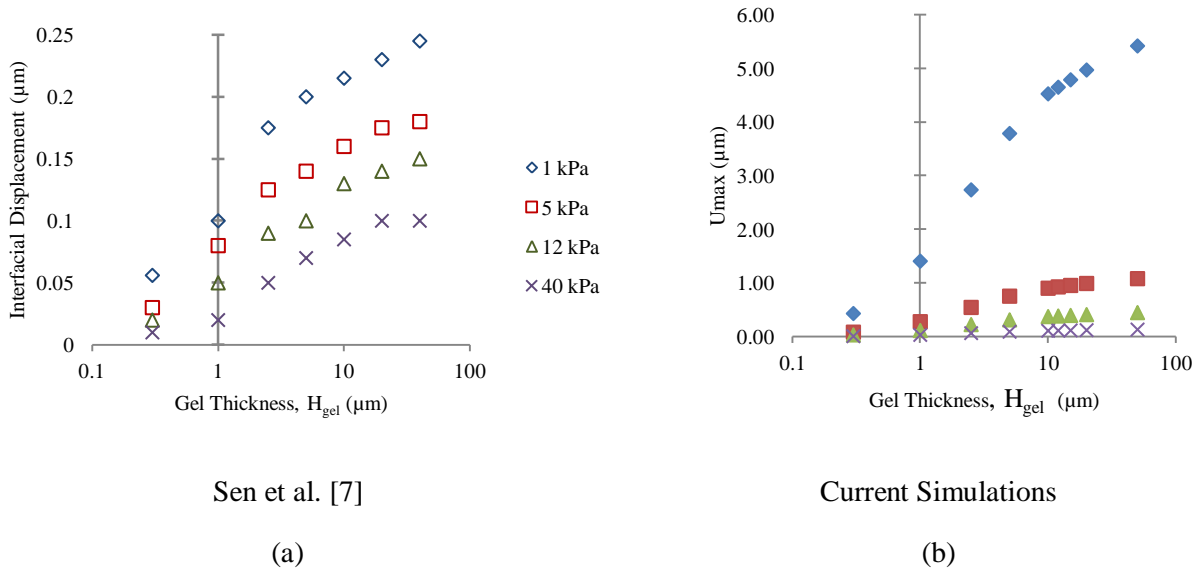
Finite Element

Linearly elastic model results

The linearly elastic model results are on a similar scale to the work of Sen et al. [7], as shown in Figure 16(a) and (b), and when normalized to results of the thickest material, closely matched the work of Sen et al. [7], as shown in Figure 16(c).

The simulated cell applying inward traction on a linearly elastic substrate of four different stiffnesses shows four different curves of maximum substrate displacement with respect to substrate thickness, as seen in Figure 16(a) by Sen et al. [7]. The curves from the model developed here are in the same order of magnitude as those obtained by Sen et al. [7] (Figure 16(b)). To better compare the data, the displacements for each stiffness are normalized to the displacement at the maximum, or infinite, thickness. As seen in Figure 16(c), the normalized interfacial displacement of the model developed here matches well with published data.

The simulations performed by Sen et al. [7] are post-processed to calculate the average interfacial strains and displacements, a process that requires requesting data on specific nodes of the model and calculating averages. It was observed that there is no statistical difference ($p > 0.05$) between maximum displacement of the model in the radial direction and average interfacial displacement, so for this project, the more time-efficient method of determining interfacial displacement - maximum displacement of the model - was used (see the Appendix, p43).

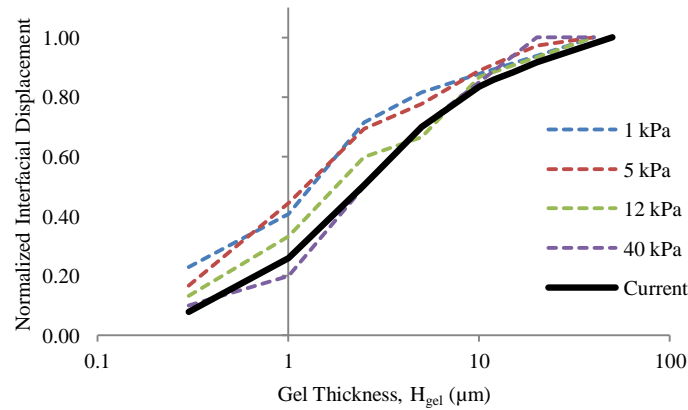


Sen et al. [7]

Current Simulations

(a)

(b)



Comparison of results from Sen et al. [7] (dashed) and current simulations (solid)

(c)

Figure 16. Agreement of this finite element model with a published model. (a) Mean interfacial displacement on gels of four stiffnesses, of various thickness, by Sen et al. [7]. (b) Maximum surface displacement from this model on gels of the same four stiffnesses, of the same various thicknesses. (c) When normalized to the displacement at the “infinitely” thick ($50\mu\text{m}$) gel, the displacements of this model align with those of the published model. The normalized displacements from all four thicknesses with this model collapse onto the black line.

Effect of thickness on substrate displacement

When the traction applied to a substrate is held constant and the thickness is changed, the linearly elastic substrate responds similarly as the stiffness changes, as shown in Figure 17(a). The largest difference in maximum substrate displacement is between 0 and 10 μm , with the response at 50 μm considered to be the response of a substrate of infinite thickness. The strain-stiffening material undergoes

a similar response, with the largest changes occurring for substrates under 10 μm thick; however, when a higher traction is applied, the strain-stiffening material behaves more like the stiffer linearly elastic substrate than when a smaller traction is applied, as shown in Figure 17(b).

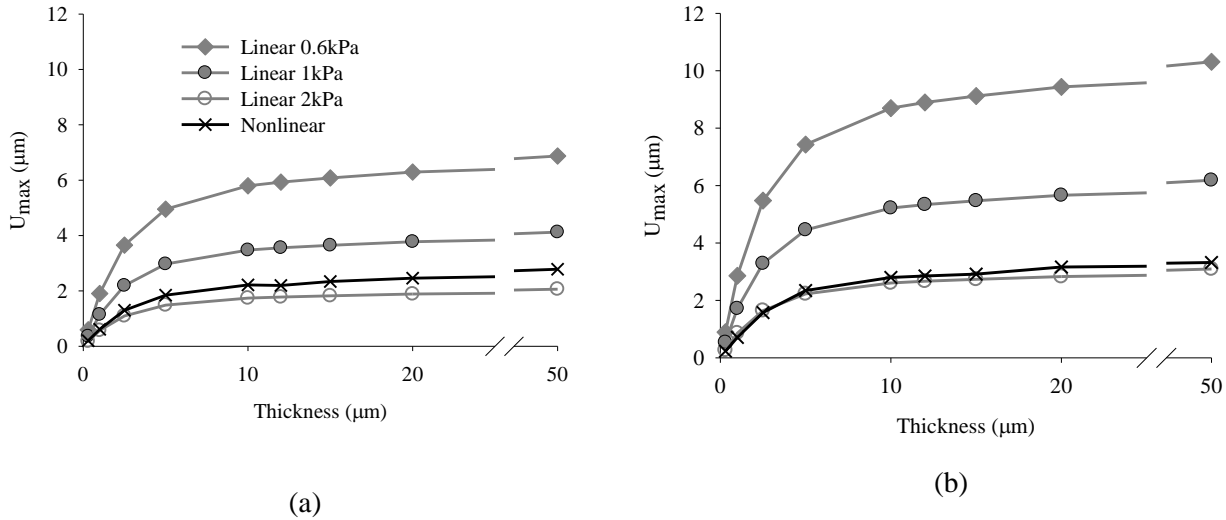


Figure 17. Substrate displacement decreases with decreasing thickness. By increasing the applied traction from 400Pa (a) to 600Pa (b), the nonlinear substrate exhibits strain-stiffening behavior by displacing like a stiffer material.

Effect of traction on substrate displacement

The effects of changing the applied traction to a substrate of “infinite” thickness were compared for models with a linearly elastic substrate of various stiffnesses and a model with strain-stiffening behavior, as shown in Figure 18(a). The maximum displacement of the linearly elastic substrate increases linearly as higher traction is applied. The substrate displacement increases proportionally as the stiffness of the material is decreased for both thin and thick substrates. The strain-stiffening material deforms by a smaller amount as the traction is increased on the surface. This behavior is seen in both the thin and thick substrates, though the thinner substrate responds more like a stiffer linearly elastic gel than the thick substrate, as shown in Figure 18(b).

Effective stiffness

To compare the effective stiffness of substrates of different thicknesses, we have used the following equation, adapted from Mehrotra et al. [23]:

$$k_{eff} = \frac{T}{U_{max}/\bar{R}} \quad (2)$$

where T is the radially-applied traction, U_{max} is the maximum substrate displacement, and \bar{R} is the mean radius of the focal adhesion area.

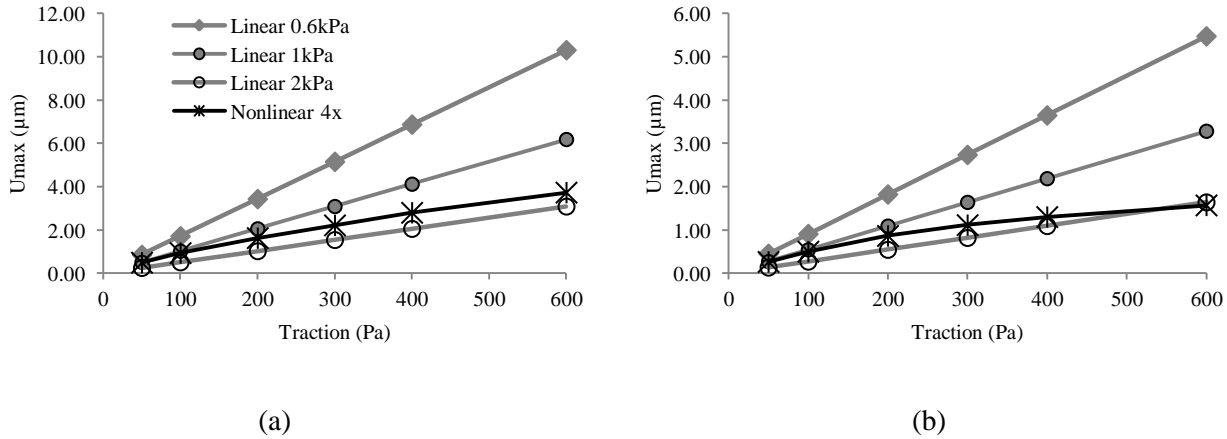


Figure 18. The maximum displacement of the top surface of linear substrates increases linearly as traction is increased. However, the nonlinear material exhibits strain-stiffening behavior; as traction increases, the ability of the nonlinear material to deform is reduced. This strain-stiffening effect is amplified by decreasing the substrate thickness from 50 μm (a) to 2.5 μm (b). On the thin substrate, the gels deform to a lesser extent than the thick gels due to the impact of the rigid boundary under the substrate.

The finite element simulations performed here indicate that the effective stiffness of a linearly elastic material decreases to a value close to the bulk stiffness within 10 μm , as shown in Figure 19(a). When the traction in the model is increased slightly but thickness is held constant, the effective stiffness of a linearly elastic material remains the same, indicating that effective stiffness is dependent on thickness alone. However, the same is not true for a nonlinear material; the effective stiffness is much higher at the thinner substrate, indicating that the response of the nonlinear material is dependent on both substrate thickness and applied traction, as shown in Figure 19(b).

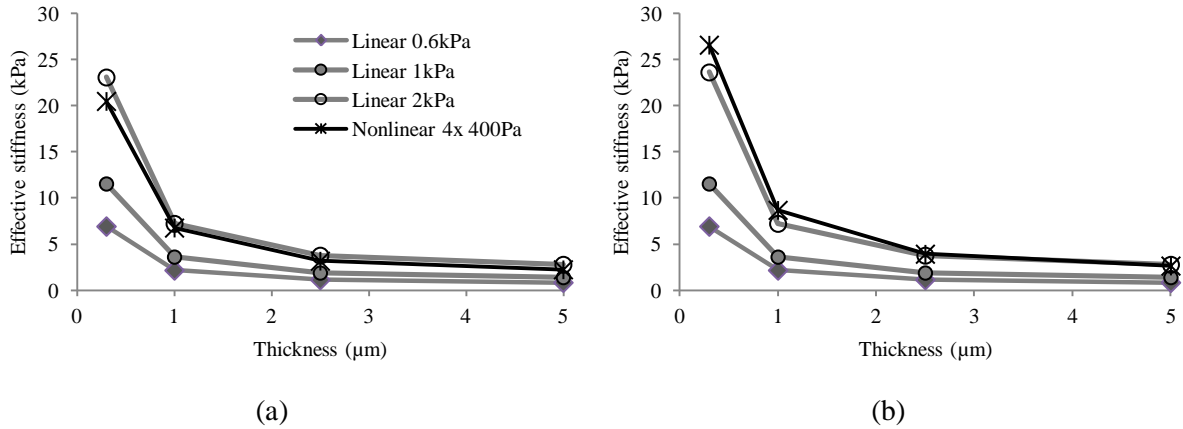


Figure 19. Effective stiffness increases sharply at low thicknesses. The strain-stiffening behavior allows the nonlinear material to become effectively stiffer at low thicknesses when the applied traction is increased from 400Pa (a) to 600Pa (b).

In Figure 20, effective stiffness is plotted versus substrate thickness and applied traction for three linearly elastic substrates and the nonlinear substrate. Note that at the highest traction, the effective stiffness of the nonlinear material goes beyond that of the linear substrates. As the traction increases, the nonlinear material experiences strain-stiffening possibly to a point where a cell’s spreading behavior would be affected.

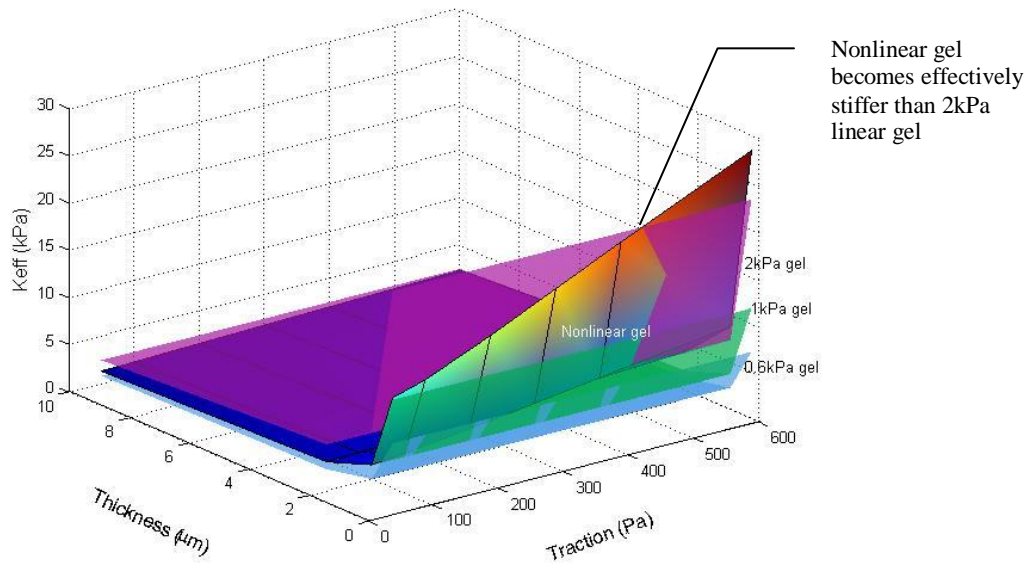


Figure 20. The impact of thickness and traction on effective stiffness of the linear and the nonlinear materials are plotted together. The stress-strain relationship of the linear materials allow the effective stiffness of these gels to be unaffected by the amount of cell-applied traction. Due to the stiffening of the nonlinear material at high strains, the effective stiffness greatly increases with increasing traction.

See the Appendix, p46 for stress and strain distributions.

Changing size and location of cell-applied traction

The defined area of cell-gel interaction is specified by Mehrotra et al. [23] with two parameters: focal adhesion radius, and width of the traction region. When the radius (R) is increased (i.e., a larger cell) or the traction region increases (i.e., more focal adhesions), the maximum surface displacement is increased. Changing the size of the cell or the size of the cell-applied traction surface also affects the effective stiffness of a linear material as shown in Figure 21. An increase in R increases the effective stiffness, while an increase in A decreases the effective stiffness. These simulations are performed on a linear elastic substrate to focus on effects of cell geometry.

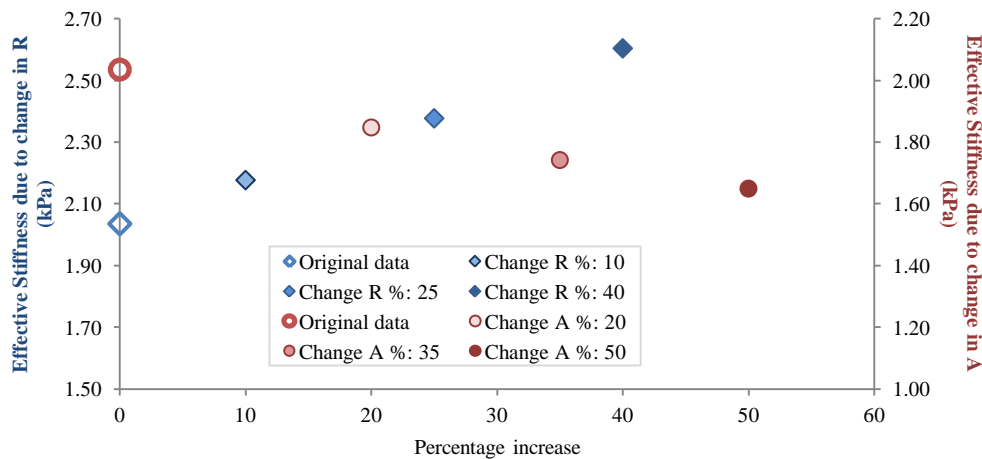


Figure 21. The effective stiffness of a linear material is dependent on the dimensions of the applied traction, and thus on the geometry of the cell. Increasing the size of the cell (R) increases the effective stiffness of the substrate. Conversely, increasing the size of the traction surface (A) decreases the substrate effective stiffness.

The above changes in R and A are performed with a constant traction (100Pa). Due to the linearity of the material, the value of the applied traction will not affect the overall response of the material. To investigate the effective stiffness response of a cell that applies the same force but only at the very edge of the cell, the model was modified to include a smaller area of cell-applied traction and a higher traction to maintain the same force as 100Pa over the original area. As shown in Figure 21, the effective stiffness of the material with this smaller area follows the same shape as that with the original area.

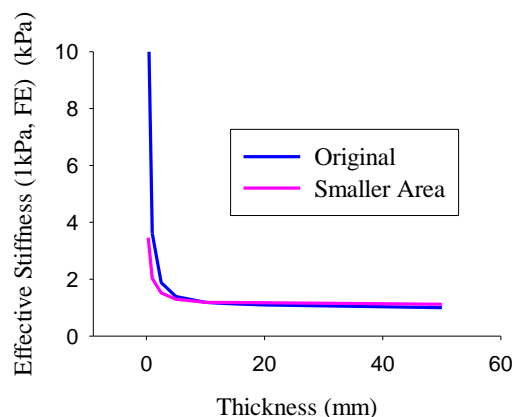
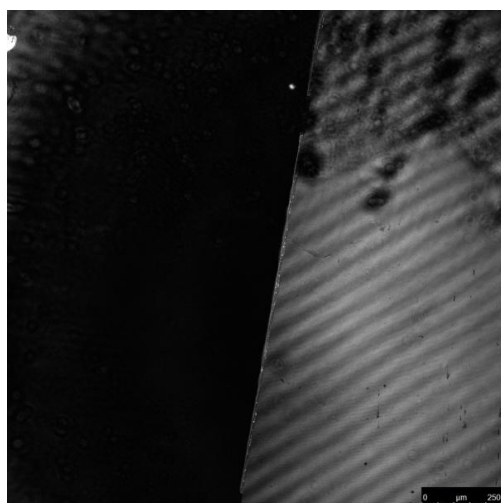


Figure 22. With the same force but a smaller area for the cell applied traction (traction \times area = constant), the linear material responds similarly to the original traction area, in terms of effective stiffness.

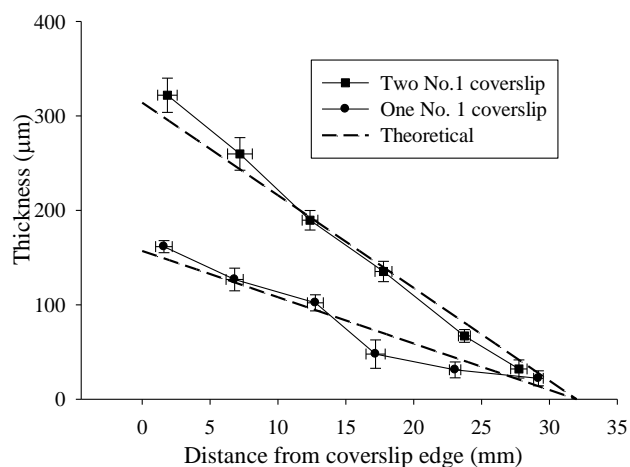
Experimental

Confirmation of Sloped Gels

To confirm the existence of the designed sloped gel and demonstrate versatility of the design, several cell-free samples of collagen gel were made with either one or two No 1 coverslips as spacers. Once the samples were mounted on the microscope, the edge of the coverslip was located, as shown in Figure 23(a), and a horizontal micrometer against the XY stage was set to zero. From this position, XZY images were obtained at several points along the length of the sample until the gel was no longer detectable, as shown in Figure 23(b).



(a)



(b)

Figure 23. Beginning at the edge of the No 1 spacer coverslip (coverslip, right; collagen gel, left) (a), thickness measurements of the gel were taken at several points along the sample and compared to the theoretical values. Reported as mean \pm SE, $n=4$ (b).

Cell spread area

Cell spreading was quantified for HLFs on sloped fibrin and sloped collagen gels, and for HLFs and 3T3s on sloped fibrin gels. The representative images in Figure 24 show the size difference of HLFs on thick (a) and thin (b) fibrin gels. The cells do not show any preferred alignment direction. Calculated cell areas for various positions every 5mm along the sloped gels are shown in Figure 25.

The HLFs on collagen are larger than those on fibrin, though the cells are from the same source. The 3T3 fibroblasts, being from a smaller species, are expectedly much smaller than the HLFs but still show the same gradual increase in area as the HLFs as the gel thickness decreases.

As shown in Figure 23(b), the minimum thickness that is measured consistently is $\sim 25\mu\text{m}$. The zero-thickness (non-control) area measurements in Figure 25 were performed on images captured from the area of the sample where no gel was visible in cross-section mode, but had been underneath the treated glass surface. For clarity, error bars are removed in Figure 26.

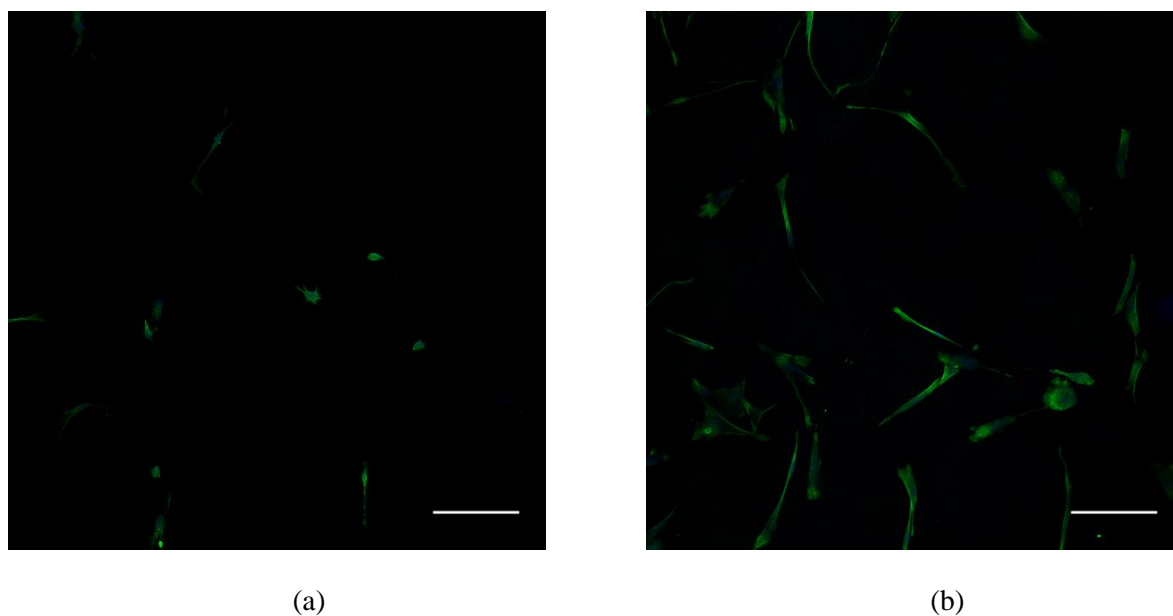


Figure 24. Representative images of HLFs on thick (a) and thin (b) fibrin gels. Scale bar = $250\mu\text{m}$.

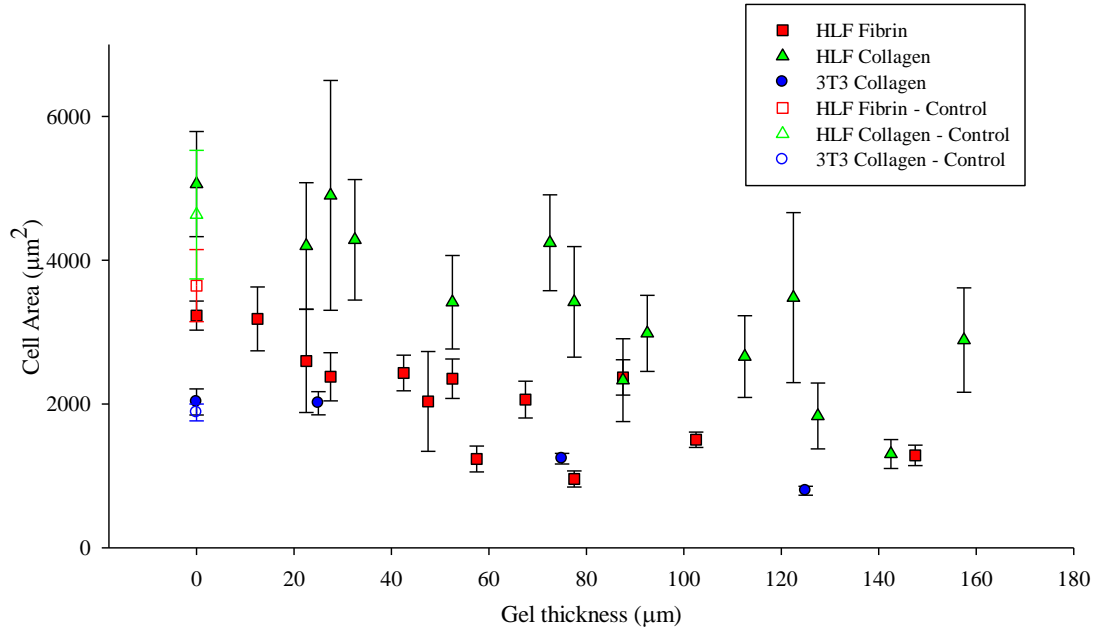


Figure 25. Cell spreading is a function of gel thickness for HLFs on fibrin and collagen gels, and for 3T3 fibroblasts on fibrin gel. Reported as mean \pm SE; HLF on collagen, mean=9 cells per data point, n=4; HLF on fibrin, mean=10 cells per data point, n=5; 3T3 on collagen, mean=44 cells per data point, n=2.

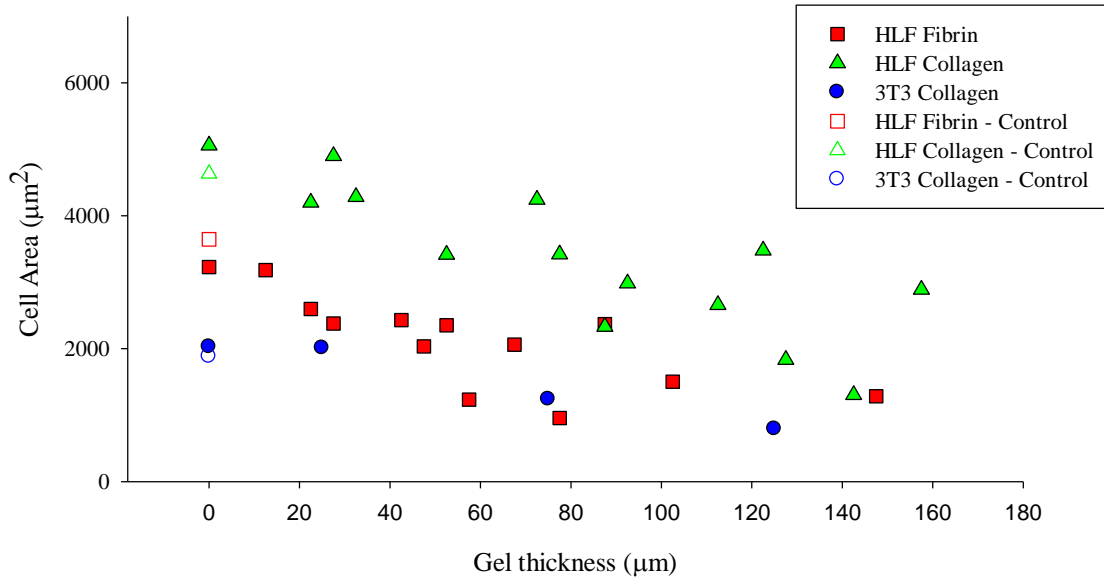


Figure 26. Cell spreading is a function of gel thickness for HLFs on fibrin and collagen gels, and for 3T3 fibroblasts on fibrin gel. Error bars removed for clarity.

Discussion

The finite element model developed in this work is a compilation of model details and experimental data from literature. The prediction of cell area based on finite element results show that the nonlinear substrate will lead to cells spreading earlier as thickness decreases compared to the finite element results from the linear substrate. However, the finite element model does not accurately capture the thickness region where experimental cells begin spreading on linear substrates, indicating that more refinement of the model is necessary.

The experimental results of two cell types on sloped gels of two protein gels show that there is much less of a sharp increase in cell area with response to perceived substrate thickness. Instead, cells on these nonlinear substrates show a more gradual area response that may be due to the cell locally stiffening the strain-stiffening material and behaving on thick substrates as they would on thin.

Finite Element

Linearly elastic model

Sen et al. [7] developed a finite element model to determine length scales of how far cells “feel” through their substrate to either a rigid underlying base or nearby cells. The cell is modeled with a contractile prestress in the cell, thus eliminating the need to model specific focal adhesions and tractions applied at those adhesions. However, the model requires the definition of cell-gel interaction, cell-membrane interaction, and cell-nucleus interaction. This model, while a good representation of cell components, unnecessarily defines a complex cell model. The cell is being defined in the finite element software, yet the interest is in the response of the substrate. A simpler model that defines a single loading condition on the surface of a substrate reduces the complexity of the model by focusing on the substrate response, and also reduces the potential variability of the cell representation.

The loading conditions and model geometry of the model described here are different than those of the finite element model by Sen et al. [7]. Validation of the linearly elastic model and comparison to

the results of the model by this group was done by normalizing the displacement values to the displacement at the “infinite” thickness (50 μm). The curves of interfacial displacement versus substrate thickness of the model by Sen et al. [7] all follow the same general shape, as seen below left, but when normalized to the displacement at the “infinitely” thick substrate, have some variation, as seen below right. The complexity of the model, which includes defining a cytoplasm and nucleus of certain size and shape, as well as a cell prestress applied to the cytoplasm only, may lead to a discrepancy in the normalized displacement-thickness curves. Reducing the complexity of the model by removing the cell entirely and focusing on the substrate response produces normalized displacement-thickness curves that are identical from one stiffness to the next, indicating that stiffness of a linearly elastic material does not play a role in the substrate response.

The amount of traction that a cell applies on a substrate spans a wide range for fibroblasts: up to 250Pa for human tendon fibroblasts (Yang et al. [26]), and up to 36kPa in 3T3 fibroblasts (Munevar et al. [20]). Since the finite element model used in this project uses an applied traction rather than a cell prestress, as in the work of Sen et al. [7], it was necessary to determine the traction value that would produce displacements on the same order of magnitude to those of Sen et al. [7]. The visualization and quantification of cell traction force of 3T3 fibroblasts via traction force microscopy, as done by Munevar et al. [20], indicates that the traction applied by a cell covers a wide range of values, with the higher tractions being toward the advancing and trailing edges of the cell.

Effective stiffness

There are several ways to quantify depth sensing or stiffness sensing of a cell, whether it be from experimental methods or computational models. Krishnan et al. [22] defined the thickness at which a cell begins to sense a rigid sub-substrate as the thickness where principal strains completely decay. In addition, this group defined an alternative definition of depth sensing as the substrate thickness where the surface deflection is less than some percentage of the deflection of an infinitely thick substrate. Maloney et al. [6] defined depth sensing as the substrate thickness that allows dissipation of adhesion site displacement and distortion of a certain percentage.

For both the linearly elastic and strain-stiffening materials, the change in substrate displacement is large between 1-20 μm and increases slower as the thickness of the substrate continues to increase. This thickness range where the surface of the substrate cannot displace as much as that of the infinitely thick material aligns with that found by Krishnan et al. [22]. The agreement of the critical thickness found by this group and the general location of the sharp increase of the effective stiffness from the finite element model defined in this work supports that this model produces results similar to those accepted in literature.

Based on the effective stiffness of the finite element simulations, the experimental setup includes sloped gels that go beyond the thickness where the material's effective stiffness will stabilize.

Predicting cell area with finite element results

Fibroblasts and human mesenchymal stem cells have been shown to have spreading behavior with increasing substrate stiffness, as well as with decreasing substrate thickness. Currently, spreading of these cell types on substrates of strain-stiffening material has not been studied. The MSCs studied by Buxboim et al. [8] were cultured on 1kPa PA gel; based on Figure 20, the area of cells on a nonlinear substrate are expected to increase earlier as substrate thickness decreases. Though this cell type is different from that modeled with the finite element simulations, these cells show the same spreading behavior as 3T3 fibroblasts on PA gel (Figure 3).

A relationship between cell area and substrate thickness is currently not in the literature for nonlinear substrates. To predict this relationship for cells on a nonlinear substrate, we used our finite element results of the substrate response for a linear, 1kPa gel and a nonlinear gel, shown in Figure 27(a), and published area and stiffness data from Engler et al. [13], shown in Figure 27(b). As seen in Figure 27(b), there is an increase in cell area as stiffness increases, with these cells more than tripling in area over a twenty-fold increase in stiffness. This increase in area as stiffness increases is expected to be present as a substrate becomes *effectively* stiffer. We combined the mathematical relationships for area-stiffness and effective stiffness-thickness, and the resulting prediction is shown in Figure 27(c). The nonlinear prediction, as we suspected, shows that the spreading begins on thicker substrates compared to

the linear prediction. However, the predictions from the finite element models reach the minimum area within $20\mu\text{m}$, whereas experimental data (Buxboim et al. [8]) shows that the cells reach minimum area closer to $60\mu\text{m}$. The equations and parameters for the curve fits can be found in the Appendix, p51.

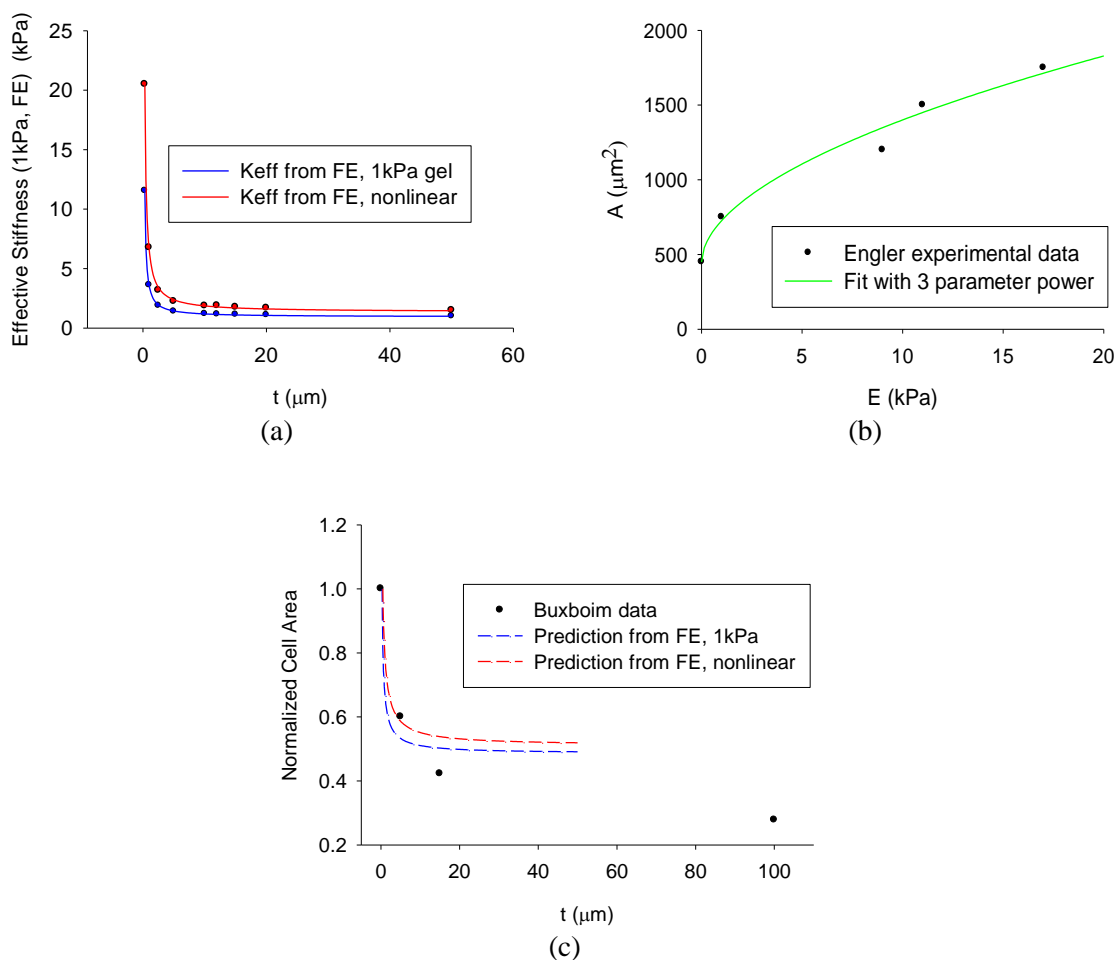


Figure 27. Prediction of cell area response to nonlinear substrate. (a) Effective stiffness from finite element simulations of linear (1kPa) and nonlinear gels show strain-stiffening of nonlinear gel at low thickness. (b) Cell area increases with increasing substrate stiffness (hMSCs on PA gel, Engler et al. [13]). (c) Comparison of predicted area to hMSCs on 1kPa PA gel (Buxboim et al. [8]). Areas are normalized to largest area to focus on trends.

Limitations of the finite element model

The finite element model defined in this work is based on cell geometry from cell imaging (Mehrotra et al. [23]), traction values from traction force microscopy (Munevar et al. [20]), and substrate geometry from a previous finite element model (Sen et al. [7]). Even with these model validations, this model and the effective stiffness definition still do not capture the spreading behavior that is indicated by

experimental data (Buxboim et al. [8]). The shape of the cell-applied traction remains the same over the course of the simulation, but fibroblasts have been shown to vary the area and magnitude of this traction (Maskarinec et al. [27]). This varying cell-applied traction is not accounted for in this finite element model, and may impact the quantification of the material response. In addition, the effective stiffness here is just one way of quantifying how stiff a material is perceived to be. A definition that can capture increasing effective stiffness at thicknesses closer to those of literature (Buxboim et al. [8]) would be needed to allow better representation of substrate response with a finite element model.

Experimental

Selection of glass surface treatments

Various surface treatments were tested to find the best for protein gel adherence and non-adherence. The three methods for protein gel adherence were: described by Bhatia et al. [28]; described by Pelham and Wang [21]; and sodium hydroxide etching with a wash of pepsin-extracted collagen (OLAF). The three methods for protein gel non-adherence were: no surface treatment; coating in Rain-X per instructions; and coating a thin layer of Sigmacote (Sigma-Aldrich). Collagen gel was polymerized between two glass slides with the same surface treatment, and each sample was rotated until the sample fell apart. If the sample was still intact, one of the glass slides was tapped against a solid edge three times with increasing pressure. The angle or tapping pressure at which the sample released was quantified for comparison.

The samples prepared with the method described by Pelham and Wang [21] remained intact better than other methods; this method was used for surface preparation of the No 1.5 coverslips for all experiments. The samples prepared with Rain-X and Sigmacote came apart easier than those on untreated glass slides; however, due to apparent cell toxicity of these materials, the top glass slides in all experiments were left untreated. See the Appendix, p53 for the results of the comparison.

Comparison of experimental cell spreading

As shown earlier in Figure 4 and Figure 25, the range of area for cell spreading spans from 500 to 7000 μm^2 . In order to compare the data between these two cell types and protein gels, the data were normalized to the area of the control for that particular experiment. The same normalization was done for data from literature. With the actual values of area ignored, we are able to see with the plots below that the two cell types behave in a similar fashion on the protein gels (Figure 28(a)). Note that error bars and controls have been removed for clarity.

The data from the work here and from literature (Maloney et al. [6], Buxboim et al. [8]) are fit to a two-parameter rational equation

$$A = \frac{a}{1+b*t} \quad (3)$$

where A is the normalized area and t is the gel thickness, shown in Figure 28. The parameter b determines the level of curvature of the equation and is used for comparison of cell response to substrate thickness (see Table 1). Higher values of b indicate that the cell area sharply increases as the substrate becomes thinner, and that the cell can “feel” the rigid boundary on these thin substrates (Figure 28(b)). In contrast, the low values of b indicate a more gradual spreading response to nonlinear substrates of decreasing thickness that is significantly different from that of the literature ($p < 0.05$).

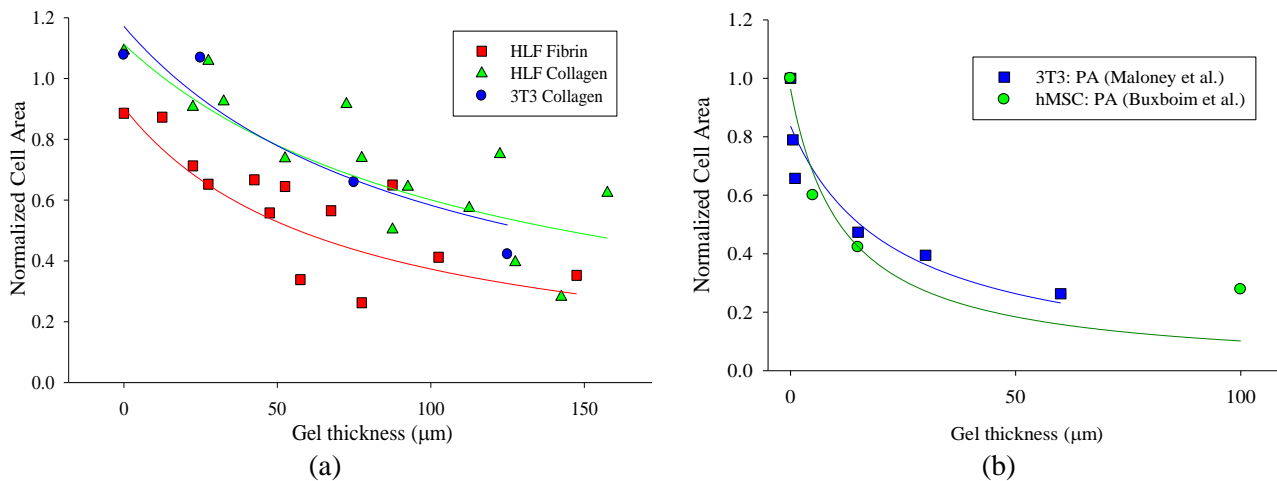


Figure 28. Comparison of area, normalized to the area at minimum thickness, of cells on linear and nonlinear substrates. (a) On PA – linear – gel, the rigid boundary under the gel is not “seen” by both 3T3 fibroblasts and hMSCs until the gels

approach thicknesses under $\sim 50\mu\text{m}$. (b) On fibrin and collagen – nonlinear – gels, fibroblasts sense the rigid boundary at gels much thicker than cells on the PA gel, and also do so in a much more gradual fashion. Note the similarity of the curves for the cells on collagen.

Table 1. Comparison of curvature (parameter b) of cell area on gels of various thicknesses. The lower values from this work mean that the area-thickness curve is less sharp than those from literature; the rigid boundary is more visible to cells on a nonlinear material.

<u>From Literature</u>	<u>From this work</u>
3T3 on PA Maloney et al. [6] 0.0435	HLF on fibrin 0.0142
hMSC on PA Buxboim et al. [8] 0.0847	HLF on collagen 0.00850
	3T3 on collagen 0.0101

Limitations of the cell experiments

The non-control zero-thickness area measurements show results similar to those from the controls (tissue culture plastic with fibrin or collagen wash), as shown in Figure 25. However, due to the adjustment of confocal software gel thickness measurements, it is difficult to accurately capture the thickness of very thin (under $\sim 15\mu\text{m}$) gels.

The cell experiments performed here show greater variability than those of published data, most likely because the number of cells analyzed is much larger in the literature. The shape factor (round, polar, multi-dendritic) of the cells could also be analyzed as a cell response to stiffness; cells that are on thicker substrates have a more round morphology than those on thin substrates. The amount of roundness as substrate thickness changes could have less variation than quantifying cell area.

In quantifying cell area, only cells with at least $50\mu\text{m}$ to the next cell were included in the calculation. This number is based on past studies of finite element simulations of depth and lateral sensing (Sen et al. [7], Buxboim et al. [8]), and though Winer et al. [9] showed substrate displacement of gel much farther from the cell on fibrin gel than on PA gel, the impact of such displacement is not clear. In addition, this distance should maintain cell isolation while allowing contact with or proximity to other cells.

Conclusion

Polyacrylamide gels provide a tunable and easily produced substrate for studying cell behavior on substrates of varying thickness or stiffness, but the linear elasticity of this material is not representative of biological tissue. Through finite element simulations and experiments done here, strain-stiffening materials have been shown to propagate the effects of a rigid boundary to a greater extent than a linear material. The impact of the nonlinearity of biological materials has not been fully realized in literature. With the knowledge gained here, it is recommended that other cell responses, such as differentiation and signaling, be studied on nonlinear materials, both in fibroblasts and additional cell types. In addition, it is recommended that the finite element model and the definition of effective stiffness be refined to allow better prediction cell area response to varying substrate thickness so that other biological materials can be simulated.

The range over which fibroblasts have shown sensing of substrate stiffness extends well into the 100-200 μm range. Designs of implants or systems that would have components in this thickness range due to space or material limitations could be impacted by this cell spreading behavior, and thus should incorporate this knowledge into the design process.

References

1. Yip CY, Chen JH, Zhao R, Simmons CA (2009) Calcification by valve interstitial cells is regulated by the stiffness of the extracellular matrix. *Arterioscler Thromb Vasc Biol* 29: 936-942.
2. Saha K, Keung AJ, Irwin EF, Li Y, Little L, et al. (2008) Substrate modulus directs neural stem cell behavior. *Biophys J* 95: 4426-4438.
3. Zhang YH, Zhao CQ, Jiang LS, Dai LY (2011) Substrate stiffness regulates apoptosis and the mRNA expression of extracellular matrix regulatory genes in the rat annular cells. *Matrix Biol* 30: 135-144.
4. Wang HB, Dembo M, Wang YL (2000) Substrate flexibility regulates growth and apoptosis of normal but not transformed cells. *Am J Physiol Cell Physiol* 279: C1345-1350.
5. Ulrich TA, de Juan Pardo EM, Kumar S (2009) The mechanical rigidity of the extracellular matrix regulates the structure, motility, and proliferation of glioma cells. *Cancer Res* 69: 4167-4174.
6. Maloney JM, Walton EB, Bruce CM, Van Vliet KJ (2008) Influence of finite thickness and stiffness on cellular adhesion-induced deformation of compliant substrata. *Phys Rev E Stat Nonlin Soft Matter Phys* 78: 041923.
7. Sen S, Engler AJ, Discher DE (2009) Matrix strains induced by cells: Computing how far cells can feel. *Cell Mol Bioeng* 2: 39-48.
8. Buxboim A, Rajagopal K, Brown AE, Discher DE (2010) How deeply cells feel: methods for thin gels. *J Phys Condens Matter* 22: 194116.
9. Winer JP, Oake S, Janmey PA (2009) Non-linear elasticity of extracellular matrices enables contractile cells to communicate local position and orientation. *PLoS One* 4: e6382.
10. Leong WS, Tay CY, Yu H, Li A, Wu SC, et al. (2010) Thickness sensing of hMSCs on collagen gel directs stem cell fate. *Biochem Biophys Res Commun* 401: 287-292.
11. Oakley C, Jaeger NA, Brunette DM (1997) Sensitivity of fibroblasts and their cytoskeletons to substratum topographies: topographic guidance and topographic compensation by micromachined grooves of different dimensions. *Exp Cell Res* 234: 413-424.
12. Semler EJ, Ranucci CS, Moghe PV (2000) Mechanochemical manipulation of hepatocyte aggregation can selectively induce or repress liver-specific function. *Biotechnol Bioeng* 69: 359-369.
13. Engler AJ, Sen S, Sweeney HL, Discher DE (2006) Matrix elasticity directs stem cell lineage specification. *Cell* 126: 677-689.
14. Flanagan LA, Ju YE, Marg B, Osterfield M, Janmey PA (2002) Neurite branching on deformable substrates. *Neuroreport* 13: 2411-2415.
15. Engler AJ, Griffin MA, Sen S, Bonnemann CG, Sweeney HL, et al. (2004) Myotubes differentiate optimally on substrates with tissue-like stiffness: pathological implications for soft or stiff microenvironments. *J Cell Biol* 166: 877-887.
16. Lo CM, Wang HB, Dembo M, Wang YL (2000) Cell movement is guided by the rigidity of the substrate. *Biophys J* 79: 144-152.
17. Engler A, Bacakova L, Newman C, Hategan A, Griffin M, et al. (2004) Substrate compliance versus ligand density in cell on gel responses. *Biophys J* 86: 617-628.
18. Yeung T, Georges PC, Flanagan LA, Marg B, Ortiz M, et al. (2005) Effects of substrate stiffness on cell morphology, cytoskeletal structure, and adhesion. *Cell Motil Cytoskeleton* 60: 24-34.
19. Solon J, Levental I, Sengupta K, Georges PC, Janmey PA (2007) Fibroblast adaptation and stiffness matching to soft elastic substrates. *Biophys J* 93: 4453-4461.
20. Munevar S, Wang Y, Dembo M (2001) Traction force microscopy of migrating normal and H-ras transformed 3T3 fibroblasts. *Biophys J* 80: 1744-1757.
21. Pelham RJ, Jr., Wang Y (1997) Cell locomotion and focal adhesions are regulated by substrate flexibility. *Proc Natl Acad Sci U S A* 94: 13661-13665.
22. Krishnan R, Oommen B, Walton EB, Maloney JM, Van Vliet KJ (2008) Modeling and simulation of chemomechanics at the cell-matrix interface. *Cell Adh Migr* 2: 83-94.

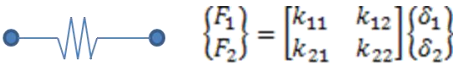
23. Mehrotra S, Hunley SC, Pawelec KM, Zhang L, Lee I, et al. (2010) Cell adhesive behavior on thin polyelectrolyte multilayers: cells attempt to achieve homeostasis of its adhesion energy. *Langmuir* 26: 12794-12802.
24. Wang N, Tolic-Norrelykke IM, Chen J, Mijailovich SM, Butler JP, et al. (2002) Cell prestress. I. Stiffness and prestress are closely associated in adherent contractile cells. *Am J Physiol Cell Physiol* 282: C606-616.
25. Franck C, Maskarinec SA, Tirrell DA, Ravichandran G (2011) Three-dimensional traction force microscopy: a new tool for quantifying cell-matrix interactions. *PLoS One* 6: e17833.
26. Yang Z, Lin JS, Chen J, Wang JH (2006) Determining substrate displacement and cell traction fields-- a new approach. *J Theor Biol* 242: 607-616.
27. Maskarinec SA, Franck C, Tirrell DA, Ravichandran G (2009) Quantifying cellular traction forces in three dimensions. *Proc Natl Acad Sci U S A* 106: 22108-22113.
28. Bhatia SN, Yarmush ML, Toner M (1997) Controlling cell interactions by micropatterning in co-cultures: hepatocytes and 3T3 fibroblasts. *J Biomed Mater Res* 34: 189-199.
29. Dembo M, Wang YL (1999) Stresses at the cell-to-substrate interface during locomotion of fibroblasts. *Biophys J* 76: 2307-2316.

APPENDIX

A brief introduction to Finite Element Analysis

Finite element analysis is a numerical method of solving complex problems by a divide-and-conquer technique. To define the model, geometry of a representative model is created, boundary conditions are assigned, and loads are applied. To solve the model, the geometry is broken into small pieces, or elements, that are connected in a network of nodes, and equations are solved for each element and combined for the final solution.

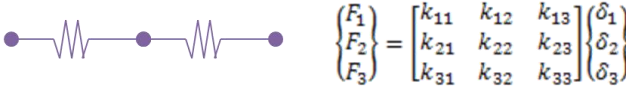
For the simplest model, a one-dimensional, one-element model, a force-displacement problem can be solved by hand.



A diagram of a single spring element represented by a zigzag line between two blue circular nodes. To the right of the diagram is the force-displacement equation:

$$\begin{Bmatrix} F_1 \\ F_2 \end{Bmatrix} = \begin{bmatrix} k_{11} & k_{12} \\ k_{21} & k_{22} \end{bmatrix} \begin{Bmatrix} \delta_1 \\ \delta_2 \end{Bmatrix}$$

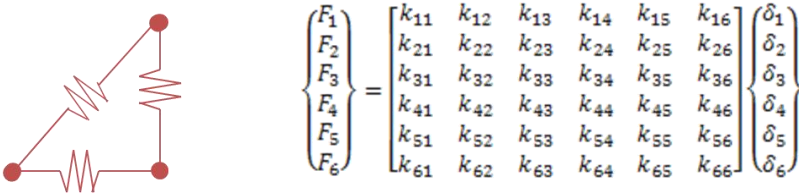
The problem becomes more complex by adding a second in-line element...



A diagram of two spring elements connected in series between three blue circular nodes. To the right of the diagram is the force-displacement equation:

$$\begin{Bmatrix} F_1 \\ F_2 \\ F_3 \end{Bmatrix} = \begin{bmatrix} k_{11} & k_{12} & k_{13} \\ k_{21} & k_{22} & k_{23} \\ k_{31} & k_{32} & k_{33} \end{bmatrix} \begin{Bmatrix} \delta_1 \\ \delta_2 \\ \delta_3 \end{Bmatrix}$$

...and quickly becomes more complex by adding a second dimension.



A diagram of a 2D truss structure with six red circular nodes and three red spring elements. To the right of the diagram is the force-displacement equation:

$$\begin{Bmatrix} F_1 \\ F_2 \\ F_3 \\ F_4 \\ F_5 \\ F_6 \end{Bmatrix} = \begin{bmatrix} k_{11} & k_{12} & k_{13} & k_{14} & k_{15} & k_{16} \\ k_{21} & k_{22} & k_{23} & k_{24} & k_{25} & k_{26} \\ k_{31} & k_{32} & k_{33} & k_{34} & k_{35} & k_{36} \\ k_{41} & k_{42} & k_{43} & k_{44} & k_{45} & k_{46} \\ k_{51} & k_{52} & k_{53} & k_{54} & k_{55} & k_{56} \\ k_{61} & k_{62} & k_{63} & k_{64} & k_{65} & k_{66} \end{bmatrix} \begin{Bmatrix} \delta_1 \\ \delta_2 \\ \delta_3 \\ \delta_4 \\ \delta_5 \\ \delta_6 \end{Bmatrix}$$

Software such as ABAQUS (Providence, RI) and ANSYS (Canonsburg, PA) solve a wide range of problems, such as stress, acoustic, or piezoelectric analyses, for a variety of materials, such as rubbers, composites, and foams. Depending on computing power, extremely complex simulations can converge

on a solution in just hours. However reasonable the solution looks, it is critical to ensure the model has been defined properly and the simulation results best match real results.

Details on the development of the Finite Element Model

Geometry

The initial model geometry was based on that by Sen et al. [7]; an axisymmetric cell-on-gel model, with the base of the gel fully constrained and contact defined between the cell and gel. Though simulations completed, determining substrate response was difficult due to the unnecessary cell geometry. To simplify the model, the cell geometry was removed from the model, allowing the simulation to focus on substrate response. Two methods of modeling a focal adhesion were tested; point load, and shear traction. The point load leads to severe element distortions, so the shear traction loading condition was chosen for all simulations.

The model geometry is based on two sources; the various substrate thicknesses are based on those used by Sen et al. [7], and the cell-gel interaction dimensions are based on Mehrotra et al. [23]. The acceptable range of tractions, as interpreted from Munevar et al. [20], is 92Pa-36kPa. Modest values for traction, 50-600Pa, were used in these simulations to remain within this range, minimize element distortions, and produce substrate displacements similar to those of Sen et al. [7].

Sen et al. [7] quantify substrate response by determining the average interfacial (cell-gel) displacement. In an effort to obtain data more efficiently from the simulations, substrate displacements determined by this averaging method were compared to the maximum substrate displacements. With an average variation of 12% of the maximum method from the average method, the maximum method is considered an acceptable method of determining substrate response.

Strain-stiffening material parameters

Modified strain-stiffening material data from Winer et al. [9] was fit to several models with the material evaluation tool in ABAQUS, and the model parameters were used in simulations increasing in complexity (axisymmetric simulations of a single-element model, followed by those with multiple

elements). To further tune the parameters, simulations with a model in pure shear were performed with test data modified from the original linear shear-axial relationship.

Incremental steps

A series of uniaxial simulations were performed with incremental changes from the linearly elastic model to ensure validity of the developing model. The strain-stiffening material behavior was defined using the incompressible linear elastic stress-strain relationship and the reduced polynomial model, while the geometry was defined first with a single element, and then multiple elements. Once the single and multiple-element simulations were in agreement, the geometry was modified to model a substrate under pure shear stress. Nonlinear materials can be defined in ABAQUS; however, shear data is not an acceptable form of input. Therefore, the original data were adjusted such that the results of the pure shear stress simulations would agree with the original rheometry data, as shown in Figure A 1.

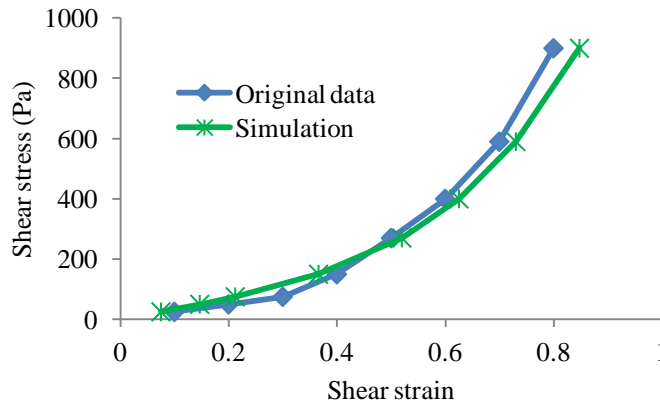


Figure A 1. The results of the simple shear simulations are compared with the original rheometry data to ensure that the fibrin gel material responds as intended.

To define the fibrin gel material property, a series of iterations were performed to verify and validate the input. As a first approximation, the incompressible linear elastic stress-strain relationship was used:

$$G = \frac{E}{2(1+\nu)} \quad (\text{A1})$$

where G is the shear modulus, E is elastic modulus, and ν is the Poisson ratio. The stress data from Winer et al. [9] were multiplied by a factor of 3 and the modified data curve was fit to several different models

using the ABAQUS material evaluation tool. The third-order reduced polynomial model was chosen and simulations were performed with this material definition. The simulations involved a simple model to recreate a gel sample undergoing testing in a rheometer. Shear traction was applied to the top surface of the rectangular geometry, while boundary conditions defined at the sides and bottom prevented vertical and any movement, respectively. The resulting shear stress and strain from these simulations were plotted and compared to the original data, and were found to have higher strains than the original data. The material data were tuned by multiplying by a factor of 4 to stiffen the material, and the simulations were run again. This material property definition better defined the material behavior when a shear stress is applied and was used for the remaining simulations.

Model variations

More “nonlinear”

In an effort to see the effect of the nonlinearity of the material on substrate displacement, the modified (4x) Winer et al. [9] (labeled as Janmey) data was made “more nonlinear” – the strain-stiffening behavior appears at a higher strain, as shown in Figure A 2(a). This material behaves much more like a softer linearly elastic material as the cell-applied traction is increased, as the material is still within the low-stress regime, as shown in Figure A 2(b). However, as the thickness is increased, the model becomes unstable, so while these simulations are not used in data analysis, it is interesting to see how the material responds to a change in definition.

Verification of the odd shape

Strain plots of the strain-stiffening material contain a “pinching” material response at the inner edge of the applied traction. To verify that this effect was not an artifact of the model, the mesh shape was changed from triangle to quadrilateral elements. As shown in Figure A 3, the pinching is apparent with both shapes. Quadrilateral elements are in the upper image; triangular elements in the lower.

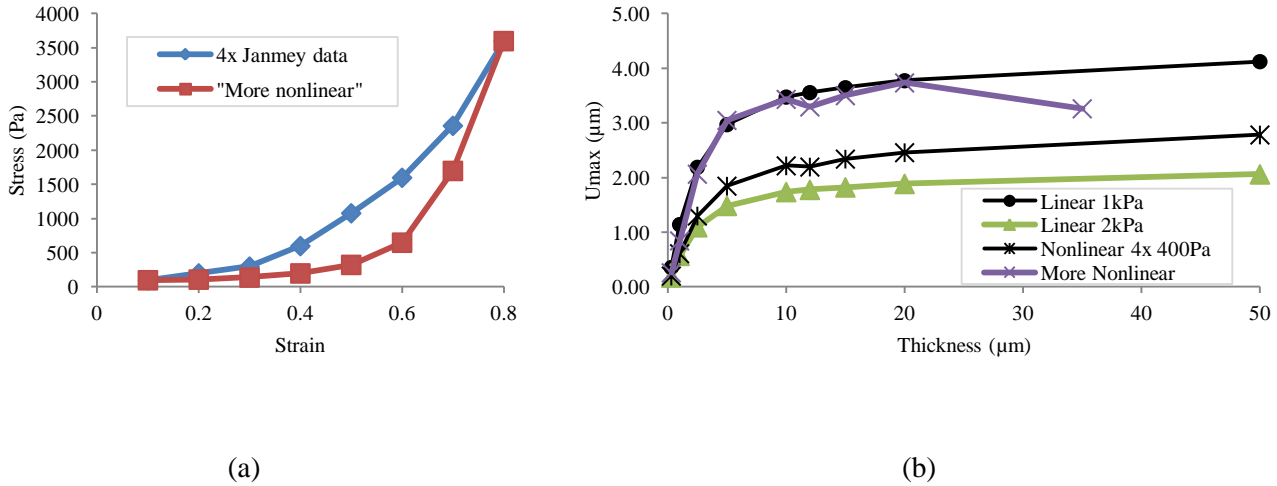


Figure A 2. (a) The nonlinear material is modified to show stiffening at higher strains. (b) The “more nonlinear” material responds much like a 1kPa gel, but the simulations begin breaking down around 10 μm .

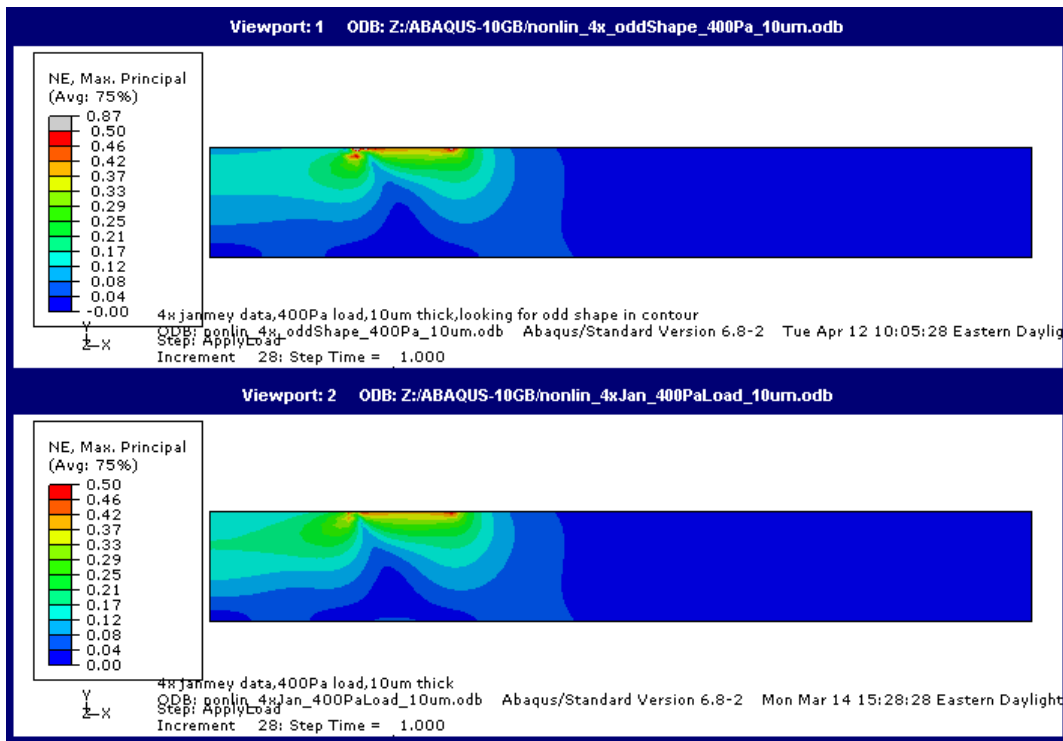


Figure A 3. The apparent pinching of the stress distribution in the nonlinear material is seen with both four-sided (above) and three-sided (below) elements.

U_{max} vs U_{avg}

Finite element analysis software provides a multitude of calculation output options, depending on the analysis type; Mises stress, displacements, temperature, electrical flux vector, just to name a few. The finite element model developed by Sen et al. [7] includes gel, cell, and nucleus structure, as well as interstructure interactions. To investigate prestress-driven matrix sensing by cells, the group obtains stress and strain distributions through the model as the prestress of the cell moves the cell-gel interface. The group also looks at the deformation of the cell-gel interface; this deformation is a representation of the work done by the cell on the matrix. The mean interfacial logarithmic strain and the mean interfacial displacement are determined for each simulation for comparison across the experiments. Similarly to this group's method, the simulations we have performed request displacement of the area modeling the cell-gel interface. However, there is no statistical difference ($p > 0.05$) between maximum displacement of the model in the radial direction and average interfacial displacement, so for this project, the more time-efficient method of determining interfacial displacement - maximum displacement of the model - was used.

Data for U_{max}, average U comparison

The following is sample displacement data collected at nodes along the top of the substrate where traction is applied. This was done for the following thicknesses: 0.3, 1, 2.5, 5, 10, 12, 15, 20, and 50 μm , as well as for the following substrate stiffnesses: 1, 5, 12, and 40 kPa

Table A 1. Displacement data of a 1kPa linear gel, 20 μ , thick, with 0.5kPa traction applied to the top surface.

20um; 1kPa stiff; 0.5kPa load

X	_temp_1	_temp_2	_temp_3	_temp_4	_temp_5	_temp_6	_temp_7	_temp_8	_temp_9	_temp_10
0	0	0	0	0	0	0	0	0	0	0
1.00E-01	-3.68E-07	-4.38E-07	-4.72E-07	-4.90E-07	-4.97E-07	-4.94E-07	-4.80E-07	-4.56E-07	-4.16E-07	-3.43E-07
2.00E-01	-7.37E-07	-8.75E-07	-9.45E-07	-9.81E-07	-9.94E-07	-9.87E-07	-9.60E-07	-9.12E-07	-8.32E-07	-6.86E-07
3.50E-01	-1.29E-06	-1.53E-06	-1.65E-06	-1.72E-06	-1.74E-06	-1.73E-06	-1.68E-06	-1.60E-06	-1.46E-06	-1.20E-06
5.75E-01	-2.12E-06	-2.52E-06	-2.72E-06	-2.82E-06	-2.86E-06	-2.84E-06	-2.76E-06	-2.62E-06	-2.39E-06	-1.97E-06
9.13E-01	-3.36E-06	-3.99E-06	-4.31E-06	-4.47E-06	-4.54E-06	-4.50E-06	-4.38E-06	-4.16E-06	-3.79E-06	-3.13E-06
1	-3.68E-06	-4.38E-06	-4.72E-06	-4.90E-06	-4.97E-06	-4.94E-06	-4.80E-06	-4.56E-06	-4.16E-06	-3.43E-06

average final U:	max:	min:
-4.45E-06	-3.43E-06	-4.97E-06

Comparison of U_{max} to Average U

Table A 2. Comparison of two methods (maximum displacement, average interaction surface displacement) for quantifying substrate surface displacement with this model.

Gel Stiffness	Gel Thickness (μm)	U _{max} (μm)	Average U (μm)	U _{max} /Average U
1 kPa	0.3	0.43	0.415	1.05
	1.0	1.41	1.19	1.18
	2.5	2.74	2.37	1.15
	5.0	3.79	3.36	1.13
	10	4.53	4.04	1.12
	12	4.65	4.15	1.12
	15	4.79	4.28	1.12
	20	4.97	4.45	1.12
	50	5.42	4.89	1.11
5 kPa	0.3	0.09	0.083	1.05
	1.0	0.28	0.238	1.19
	2.5	0.55	0.474	1.16
	5.0	0.76	0.672	1.13
	10	0.91	0.808	1.12
	12	0.93	0.831	1.12
	15	0.96	0.856	1.12
	20	0.99	0.891	1.12
	50	1.08	0.979	1.11
12 kPa	0.3	0.04	0.035	1.05
	1.0	0.12	0.099	1.18
	2.5	0.23	0.198	1.16
	5.0	0.32	0.280	1.13
	10	0.38	0.337	1.12
	12	0.39	0.346	1.12
	15	0.40	0.357	1.12
	20	0.41	0.371	1.12
	50	0.45	0.408	1.11

40 kPa	0.3	0.01	0.010	1.05
	1.0	0.04	0.030	1.19
	2.5	0.07	0.059	1.16
	5.0	0.09	0.084	1.13
	10	0.11	0.101	1.12
	12	0.12	0.104	1.12
	15	0.12	0.107	1.12
	20	0.12	0.111	1.12
	50	0.14	0.122	1.11

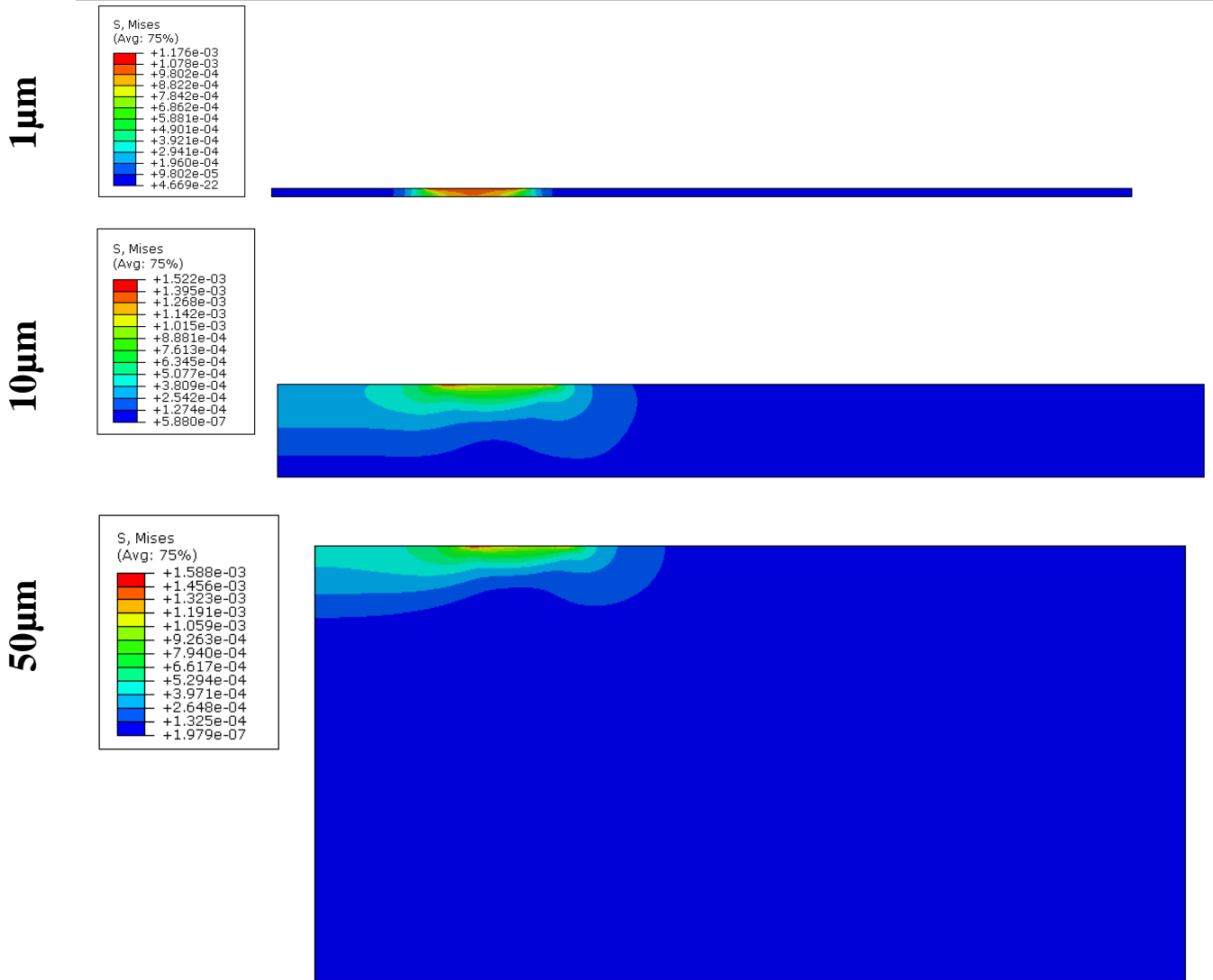
<i>U_{max}/Average U</i>	
1.05	MIN
1.19	MAX
1.12	MEAN
0.035	standard deviation
0.731	t-test

Stress and strain distributions

Comparison of von Mises stress and strain distribution in linear and nonlinear gels. Thicknesses: 1, 10, 50 μm ; traction applied at top surface: 600Pa. All distributions are plotted on undeformed geometry.

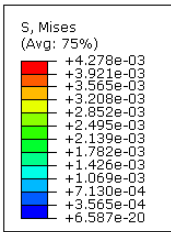
Stress distributions

Linear (1kPa) stress distributions

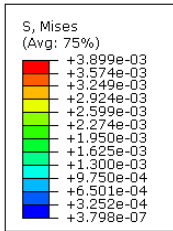


Nonlinear (fibrin) stress distributions

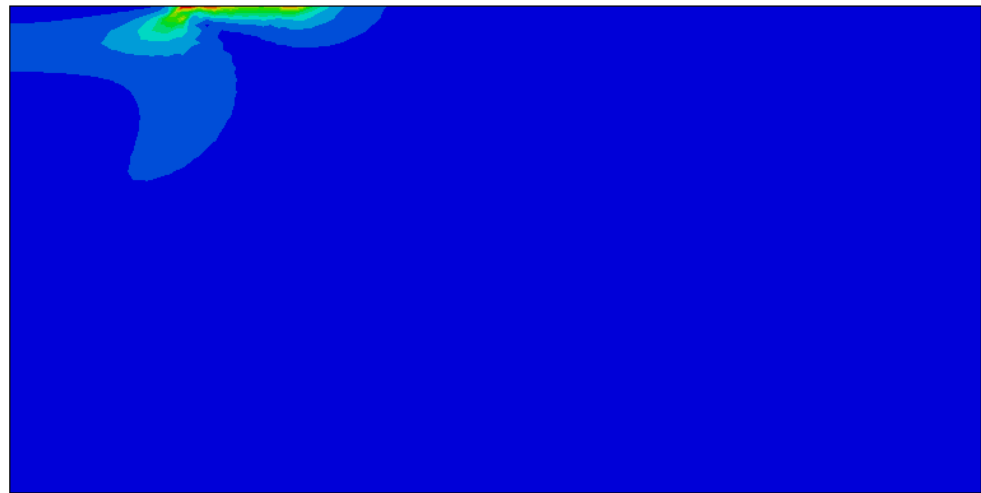
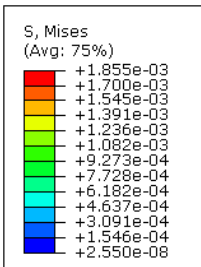
1μm



10μm

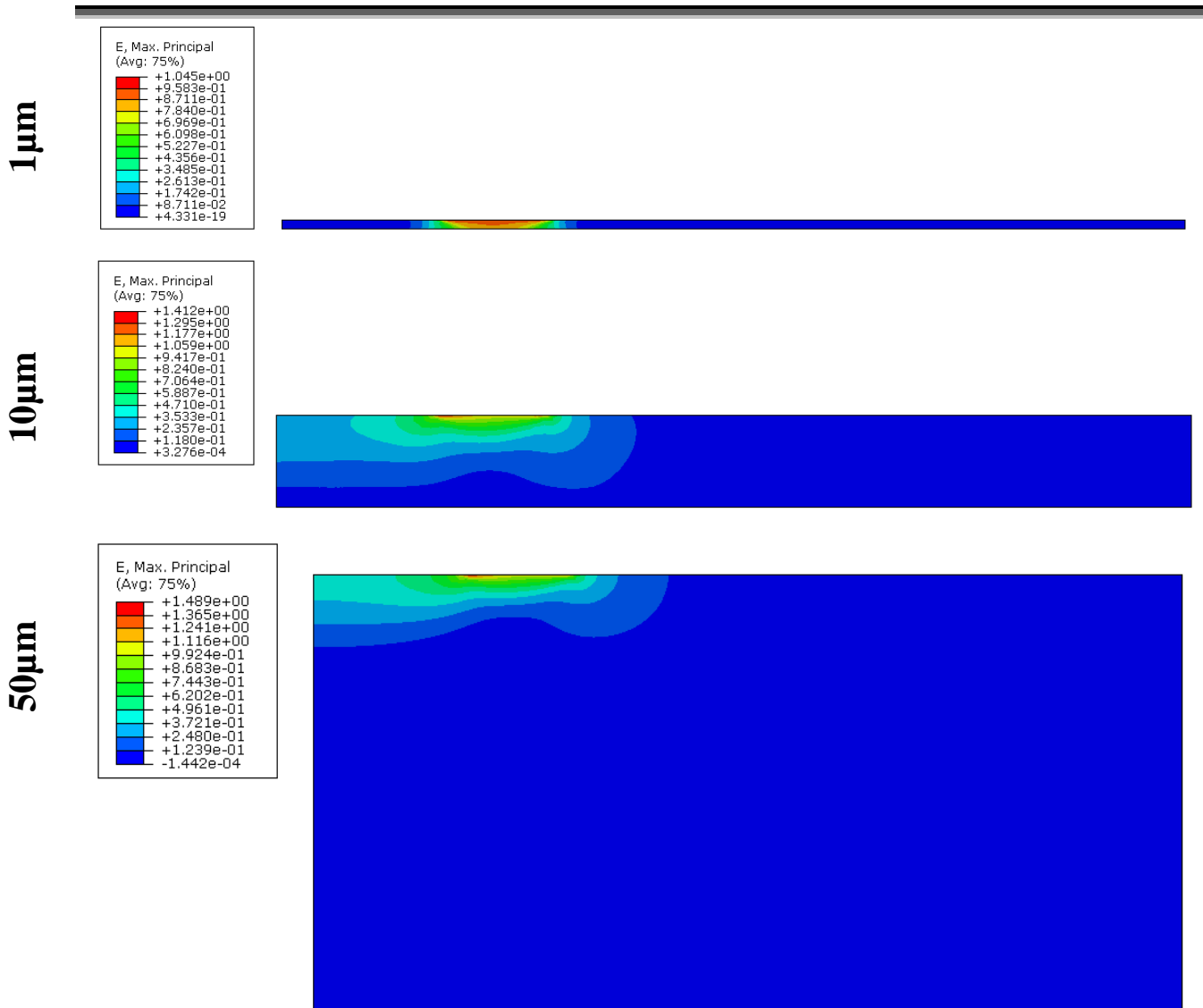


50μm



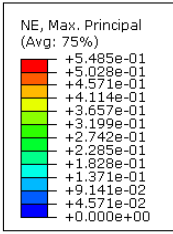
Strain distributions

Linear (1kPa) strain distributions

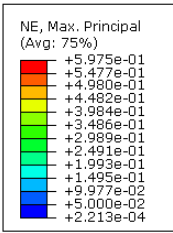


Nonlinear (fibrin) strain distributions

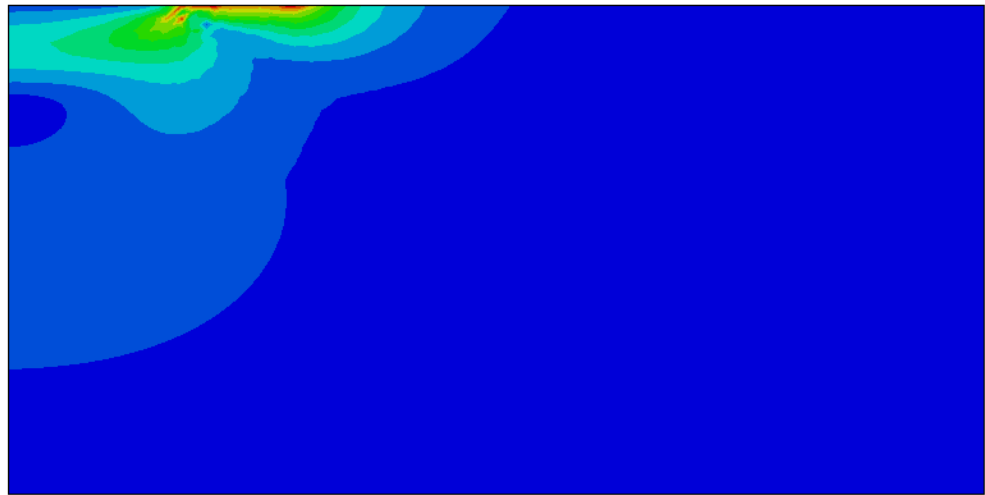
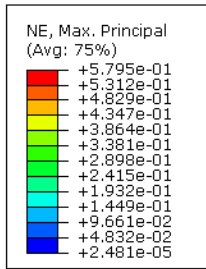
1 μ m



10 μ m



50 μ m



Quantitative Comparison of Stress and Strain Distributions

From the above images of stress and strain contour plots of cell-applied traction on linear and nonlinear materials, we see that the stress in the nonlinear material does not travel as far as that in the linear material. In contrast, strains are transmitted further through the nonlinear than in the linear material.

For a quantitative comparison, two distances on the undeformed contour plots were measured for materials of “infinite” thickness ($50\mu\text{m}$). The lateral distance from the outer point of the cell-applied traction to the farthest contour line was measured for strain and Von Mises stress for both materials. These variables were also quantified by measuring the vertical distance from the top surface to the farthest contour line along the axis of symmetry. This farthest contour line is the region where the variable is roughly 8% of the local maximum, representing stress or strain that has attenuated to that of the bulk material. The distances are shown in Table A 3. Note the larger distance to the farthest strain contour and the shorter distance to the farthest stress contour of the nonlinear material compared to the linear material.

Table A 3. Comparison of distances between outer edge of cell-applied traction (lateral) or centermost region of the top surface and the farthest contour line.

		<i>Distance to farthest contour (μm)</i>	
		Linear (1kPa)	Nonlinear
Strain	<i>Lateral</i>	8.96	16.4
	<i>Vertical</i>	8.21	37.5
von Mises stress	<i>Lateral</i>	8.21	6.94
	<i>Vertical</i>	8.21	6.88

Area prediction from FE results

In Figure 27(a), the effective stiffness-gel thickness relationship from the FE models (1kPa linear, nonlinear) are fit with a two-parameter rational equation

$$K_{eff} = K_{eff0} + \frac{1}{c + dt} \quad (A2)$$

where K_{eff0} is the effective stiffness, t is the gel thickness, and c and d are parameters with the following values:

	1kPa linear	Nonlinear
K_{eff0}	0.9405	1.353
c	-0.02800	-0.006700
d	0.4079	0.1963

The effective stiffness of the linear material when it is “infinitely” thick is 1.7kPa, while the Young’s modulus of this material is defined as 1kPa. To relate the effective stiffness and actual stiffness, E , a factor of 1.7 is applied to the linear effective stiffness values, and for consistency, is applied to the nonlinear effective stiffness values.

$$K_{eff} = 1.7E \quad (A3)$$

Our goal is to predict cell area from the effective stiffness results of the FE models. The spreading of hMSCs as PA gel stiffness increases is reported by Engler et al. [13]. For the prediction, these data are fit to a three-parameter power equation

$$A = A_0 + a * E^{-b} \quad (A4)$$

with the following parameters:

A_0	449.9
A	276.5
b	0.5632

The above equations are combined to predict cell area from FE effective stiffness and thickness values

$$A = A_0 + a \left[\frac{1}{1.7} \left(K_{eff_0} + \frac{1}{c + dt} \right)^{-b} \right] \quad (A5)$$

Experimental details

Glass surface treatments

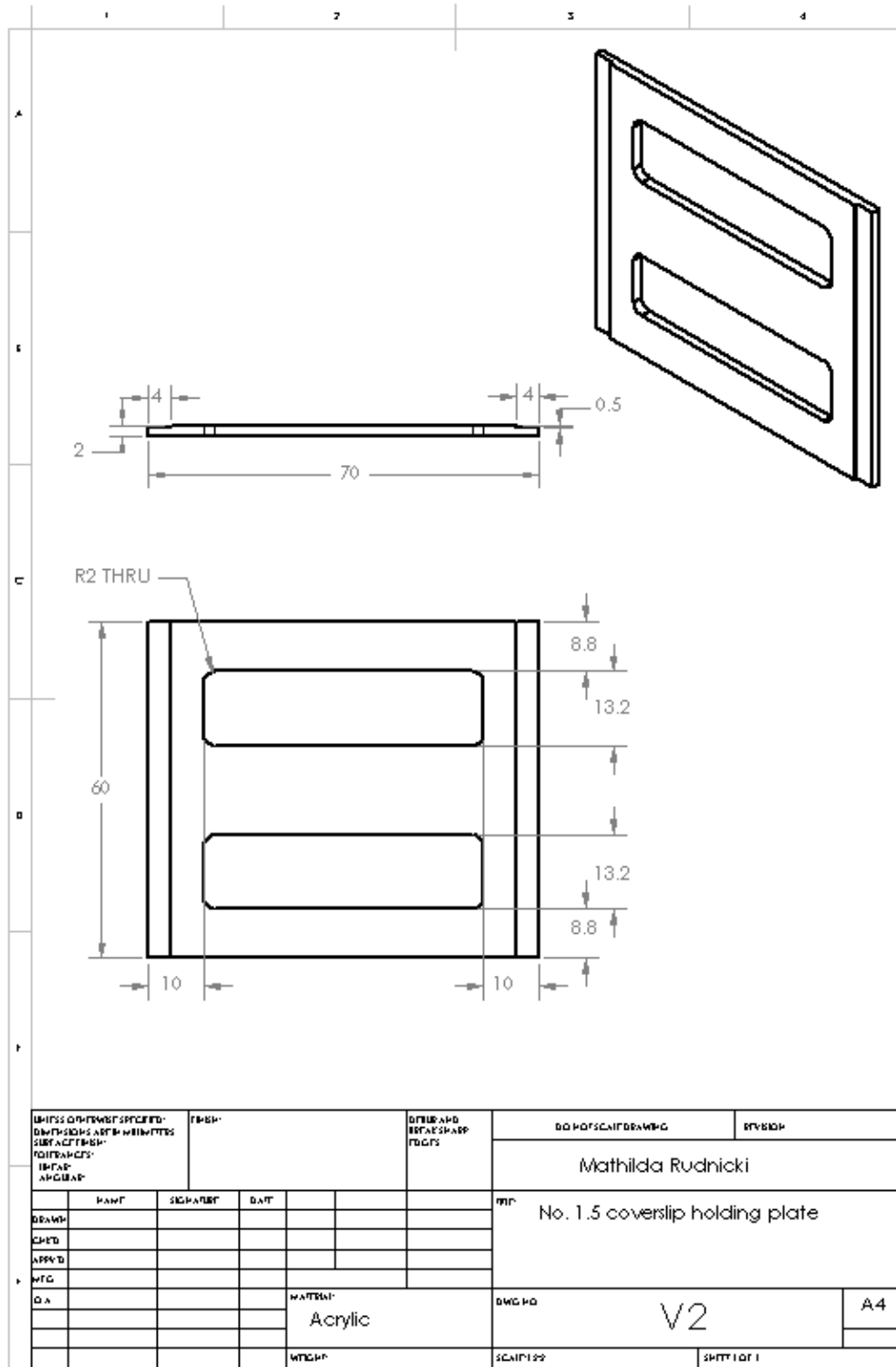
Table A 4. Comparison of various glass surface treatments for adhesion, non-adhesion of collagen gel.

Treatment	Sample	Falls off with rotation? (deg)	Falls off with tapping? (pressure)
Bhatia et al. [28]	1	No	Medium
	2	15	---
Pelham and Wang [21]	1	No	Hard
	2	No	Hard
Sodium Hyrdoxide + Collagen	1	15	---
	2	No	Medium
Untreated	1	45	---
	2	80	---
Rain-X (per instructions)	1	15	---
	2	15	---
Sigmacote (per SL-2 product information sheet)	1	5	---
	2	10	---

Creating PA gels and culturing cells

To produce these PA gels, acrylamide, bis-acrylamide are crosslinked with tetramethylethylenediamine (TEMED) and ammonium persulfate. By varying the amount of acrylamide and bis-acrylamide, various stiffnesses can be obtained. The thickness of the gel, when used for cell culture, is generally controlled by applying a silanized coverslip to the gel solution: the shape of the gel is produced by forming the gel between a glass slide and coverslip. Cells do not bind to PA gel, so the surface must be conjugated with collagen by the application of Sulfo-SANPAH ((sulfosuccinimidyl 6 (4-azido-2-nitrophenyl-amino) hexanoate)) (Dembo and Wang [29]).

Solidworks drawing of acrylic holder for No 1.5 coverslips



Confocal/micrometer measurement discrepancy

The thickness measurements of No 1.5 and No 1 coverslips, as physically measured with a micrometer, do not align with the confocal software measurements of these same coverslips. To account for this difference in refractive indices, the confocal software measurements of gel are multiplied by a factor of 1.5 for all reported thicknesses.

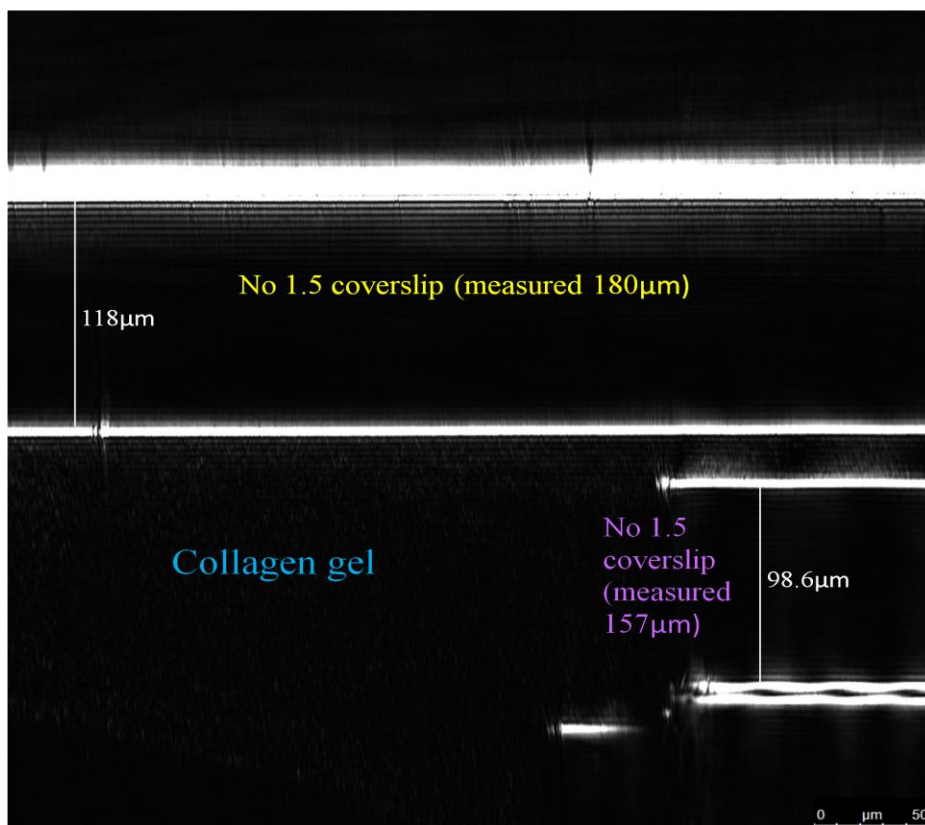


Figure A 4. The software measurements, in white, are consistently smaller than the physical measurements of the coverslips, in yellow and purple, by a factor of 1.5.

Protocols

General protocol for sample construction

1. Activate No 1.5 coverslips
2. On underside of No 1.5 coverslip, mark the ID number (thick side) and draw a mark 1cm from the opposite edge (thin side).
3. Glue No 1 coverslips to No 1.5 coverslips with silicone surgical glue, ensuring edges align. This will be the thick side of the sample.
4. Make protein gel and pipette ~0.5mL onto No 1.5 coverslip.
5. Align the edge of the top glass slide with the mark from step 2, and carefully lower onto the gel solution. Once in place, gently lower a 50g mass onto the top glass slide.
6. Allow gel to polymerize for appropriate time.
7. In the culture hood, prepare the 100mm dishes by placing 2 No 1 coverslips per sample on one side (two samples per dish).
8. Gently remove the sample from the top slide and place in dish with the thin side atop the No 1 coverslips.
9. Place down hockey walls, cover samples with prewarmed media until you are ready for cell seeding.
10. Aspirate media from sample, seed cells, and incubate overnight.
11. Fix with 4% paraformaldehyde, stain with phalloidin, and stain with Hoechst.
12. Using a normal tip transfer pipette, draw a bead of rubber cement around each opening of the acrylic holders.
13. Remove the hockey walls from the samples, and gently place samples on acrylic holders, gel facing down.
14. Protect samples from light, and allow rubber cement to dry (5-10minutes).
15. Overturn samples and cover gel with mineral oil.
16. Check for leaks before mounting on confocal microscope.

Glass Activation Protocol 5.0

Source: (Modified from) Yu-li Wang Laboratory

August 8, 2011

Materials:

- Ethanol burner with ethanol
- Glass slides to activate
- Cell scrapers
- NaOH, 0.1N, 100 ml – mix in fume hood – [bases cabinet](#)
- 3-aminopropyltrimethoxy silane - Acros, 31325100 – [flammables cabinet](#)
- 1x PBS
- Glutaraldehyde, 0.5% (prepared) in PBS (stock glutaraldehyde, Electron Microscopy Sciences, 70% solution, EM grade cat#16360) – mix in fume hood
- Dishes for rinsing

Glass Activation:

Make sure you keep track of which side is being activated!! (tip: [keep activated side up](#))

1. Pass one side of a slide over inner flame of ethanol burner, place flamed side up on benchtop.
2. Once cool, transfer to a glass dish lined with absorbent liner. (The NaOH will react with an Aluminum rack.)
3. Using a plastic pipet in the chemical hood, cover the flamed side of the slides with 0.1N NaOH and spread with the NaOH cell scraper. Let sit under fume hood until dry (2-4 hrs).
4. Using a glass pipet in the chemical hood, add 6-8 drops of 3-aminopropyltrimethoxy silane on the NaOH sides of the slides, and spread with the silane cell scraper.
5. Incubate for 5 minutes at room temp
6. Place slides in dish with distilled water, treated side up. Shake for 20-60 minutes, changing the water 3x (minimum) at room temp or until the slides are clear (NaOH waste container). There will be a clear thick substance on glass – this should be rinsed off completely before continuing!!!

(It is important to rinse well at this step, otherwise the slips will have a reddish tint after application of gluteraldehyde).

7. Under the fume hood, add 6-8 drops of 0.5% gluteraldehyde, and spread with glut. cell scraper. Incubate for 30 minutes at room temp.
8. Place slides in rinsing dishes, add distilled water, and shake for 20-60 minutes, changing the water 3x (minimum) at room temp or until the slides are clear.
9. Dry slides vertically on plastic test tubes racks to prevent water marks. Remember which side is activated!
10. Store at room temp.

Collagen gel protocol

Materials (for ~1mL):

- 40mL NaOH (0.1N)
- 200mL 5x DMEM
- 800mL collagen of desired concentration

Collagen gel preparation:

1. Add NaOH, DMEM to eppendorf tube with pipet.
2. Add collagen with 1mL syringe, triturate slowly until homogeneous.
3. With 1mL syringe, drop collagen solution slowly into/on surface.
4. Allow to polymerize ~1hr at room temperature.
5. To store, cover in PBS and store at 4°C. Gels will keep 1-2 days.

Fibrin gel protocol

Materials (for ~5mL):

- 3.75mL HBSS
- ½ aliquot fibrinogen (0.75mL)
- 1mL 1X DMEM
- 3.75µL 2N Ca²⁺
- 50µL thrombin

Fibrin gel preparation:

1. Label two 15mL conical tubes, one F, one T.
2. In tube F, add HBSS and fibrinogen
3. In tube T, add DMEM, 2N Ca²⁺, and thrombin
4. Pipette contents of T into F and triturate slowly.

Hockey wall dimensions

These small rectangular frames cut from a silicone sheet are placed on top of the gel samples just prior to cell seeding and minimize cell suspension migration off the gel.

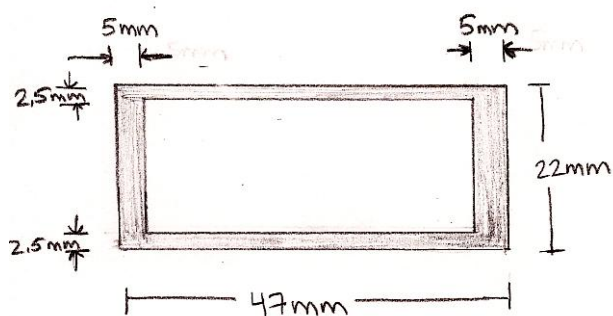


Figure A 5. Dimensions for the silicone frames used to contain the cell suspension on the sloped gels.

Image analysis

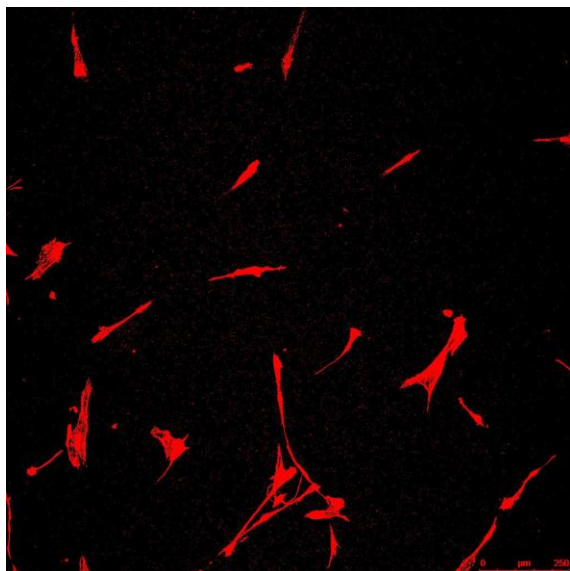
ImageJ thresholding steps

- In ImageJ, set the scale for the objective used, as in Table A 5:

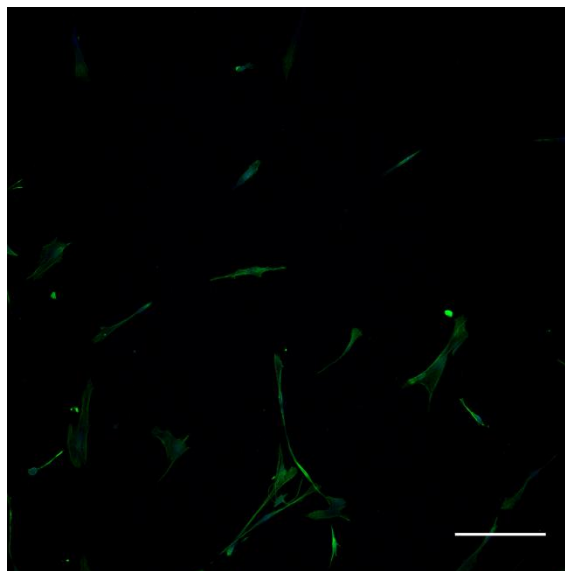
Table A 5. Image scales for different objectives and resolutions.

Leica Confocal		Leica Upright	
Mag, resolution	$\mu\text{m}/\text{pix}$	Mag, resolution	$\mu\text{m}/\text{pix}$
10X, 1024x1024	1.52	10X, 1024x1024	0.505
10X, 512x512	3.03		
20X, 1024x1024	0.758		
20X, 512x512	1.52		

- Adjust the threshold (Image: Adjust→Threshold) with the top slider for brightness so that the thresholded cells (Figure A 6(a)) match the original image (Figure A 6(b)).



(a)



(b)

Figure A 6. The thresholded image (a) is visually compared to the original image (b) to ensure that ImageJ will appropriately calculate the area of the phalloidin-stained fibroblasts.

- Analyze the image (Analyze: Analyze Particles). Set the size to 200-infinity, deselect Exclude on Edges, and select Include Holes.

- Remove measurements for cells for the following reasons:
 - a. Less than 50 μ m to the nearest cell
 - b. Multiple nuclei
 - c. Thresholded cell does not match original image well
- Save the results in a text file for the MATLAB code.

MATLAB code

This code is used on the results from the particle analysis in ImageJ. The code will write the cell areas of the desired measurement files to a file, and report the mean and cell count.

```
% This code is used to calculate average cell area from manual tracing in
% ImageJ. The filenames are of the syntax "area_manual_trace_imageID,"
% where imageID refers to the sample number, area number, thickness,
% objective, stain, and trial (ie 26t40p1 is the 2nd sample, 6th area,
% thin, 40x, phalloidin, 1st in the group)
```

```
%% Initialize
```

```
clear; clc; close all;
cellCount=0;
```

```
%% Import data
```

```
writeName=input('Filename to write cell area? ', 's');
% writeNo=input('Filename to write cell number? ', 's');
numImage=input('How many images at this magnification? ');
```

```
for i=1:numImage
```

```
    getName=input('What is the image name? ', 's');
    fileName=strcat('area_trace_', getName, '.txt');
    data=dlmread(fileName, '\t', 1, 0);
    cellNo=size(data, 1); %Number of cells averaged
    area=data(:, 2); %Area data from cell tracing
    dlmwrite(writeName, area, '-append');
    cellCount=cellCount+cellNo;
```

```
end
```

```
cellArea=dlmread(writeName); %read area data, written in for loop
avgArea=mean(cellArea); %calculate average area
dlmwrite(writeName, cellCount, '-append'); %append cell count to file
dlmwrite(writeName, avgArea, '-append'); %append average area to file
```

```
disp(['The number of cells counted is: ', num2str(cellCount)]);
disp(['The average cell area is: ', num2str(avgArea), 'um^2']);
```